NASA CONTRACTOR REPORT

EXPERIMENTAL RESULTS AND DATA ANALYSIS TECHNIQUES OF A HYDROGEN-FUELED SUPERSONIC COMBUSTOR

by C. L. Yates, F. S. Billig, and G. L. Dugger

Prepared by
JOHNS HOPKINS UNIVERSITY
Silver Spring, Md.
for

NATIONAL AERONAUTICS AND SPACE ADMINISTRATION • WASHINGTON, D. C. • AUGUST 1966

[redacted]

NASA CR-531

EXPERIMENTAL RESULTS AND DATA ANALYSIS TECHNIQUES OF A HYDROGEN-FUELED SUPERSONIC COMBUSTOR

By C. L. Yates, F. S. Billig, and G. L. Dugger

[redacted]

NOFORN

[redacted]

[redacted]

Prepared under Contract No. SC-R-76/21-09-001 by
JOHNS HOPKINS UNIVERSITY
Silver Spring, Md.

for

NATIONAL AERONAUTICS AND SPACE ADMINISTRATION

[redacted]

EXPERIMENTAL RESULTS AND DATA ANALYSIS TECHNIQUES OF A HYDROGEN-FUELED SUPERSONIC COMBUSTOR+

C. L. Yates, F. S. Billig and G. L. Dugger

Applied Physics Laboratory
The Johns Hopkins University*
Silver Spring, Maryland

ABSTRACT

An analytical technique (based on concentric streamtubes at the exit plane) for describing the non-uniform, exit flow field of a hydrogen-fueled supersonic combustor is described and shown to give satisfactory results when applied to actual experimental data. The experimental program is being conducted with a conical combustor to which arc-heated air is supplied at Mach 2.95, 2000°R and 11 psia for periods of 25 to 30 sec. The combustor has a 2.7-in. inlet diameter, an exit-to-inlet area ratio of 2 and a length of 20.5 in. Heated hydrogen is injected at the walls either normal to or partially downstream to the airstream from either an annular slot or discrete holes. The experimental setup and instrumentation are fully described. Results show that combustion efficiency is very sensitive to injector geometry, fuel temperature and equivalence ratio,

+ This research supported by NASA, Office of Aeronautical Research, Advanced Research and Technology under Contract SC-R-76/21-09-001.

* Operating under Contract NOw 62-0604-c with the Bureau of Naval Weapons, Department of the Navy,

NOMENCLATURE

A	Area, ft^2
C_P	Pressure coefficient
c_P	Specific heat, $Btu/lb_m\text{-}^oR$
S	Stream thrust, lb_f
f_s	Stoichiometric fuel-air ratio
H	Sensible enthalpy, Btu/lb_m
ΔH	Heat of formation, Btu/lb_m
h	Absolute enthalpy, Btu/lb_m
Δh	Sensible heat, Btu/lb_m
M	Mach number
$\mathfrak{M}$	Molecular weight, $lb_m/lb\text{-mole}$
n	Mole number
P	Pressure, lb_f/ft^2
p_t'	Pitot pressure, lb_f/ft^2
$\dot{Q}$	Heat flow rate, Btu/sec
q	Dynamic pressure, lb_f/ft^2
R	Universal gas constant, 1545.3 $ft\text{-}lb_f/lb\ mole\text{-}^oR$
T	Temperature, ^oR
V	Velocity, ft/sec
v	Volume, ft^3
w	Weight, lb_m
$\dot{w}$	Weight flow rate, lb_m/sec
X	Mole fraction
Y	Mass fraction

α	Combustor divergence half-angle, measured from horizontal, degree
β	Fuel injection angle, measured from horizontal, degree
δ	Cone static probe half-angle, degree
η_c	Combustion efficiency
γ	Specific heat ratio
λ	Conversion factor = 2.504×10^4 lb_m-ft^2/Btu-sec^2
φ	Equivalence ratio
ρ	Density, lb_m/ft^3 or slug/ft^3
τ	Frictional shearing stress, lb_f/ft^2
θ	Momentum flux, lb_f/ft^2

Subscripts

a	Air
b	Gas sample bottle
c	Combustor
cp	Combustor products
e	Combustor exit
eff	Effective
f	fuel
g	Gas sample
i	Combustor inlet
K	Calorimeter
S	Cone static probe surface
t	Total conditions
w	Combustor wall conditions or calorimeter quenching water conditions
∞	Free stream conditions

1	Combustor inlet
2	Fuel exit
3	Combustor. exit
4	Calorimeter quenching water inlet
5	Calorimeter exit

Superscript

*	Conditions at M = 1.0

ILLUSTRATIONS

Figure

TABLES

INTRODUCTION

The weight limitations apparent in man's initial conquest of space using rocket-powered boosters have naturally stimulated the scientific community to find a more efficient second generation accelerator. Theoretical analyses invariably conclude that the ultimate chemical propulsion system will be, at least in part, a supersonic combustion ramjet using hydrogen fuel (see, e.g., Refs. 1-6). Recognition of this attractive potential has led to a desire to obtain the data needed to specify the design of efficient injection and combustion systems, and to experimentally verify the expected combustor performance. In pursuing this goal, a prime requirement is to gain understanding of the basic phenomena that control the supersonic mixing and combustion of H_2 and air in order to identify critical parameters and determine their relative importance (see, e.g., Refs. 7-10). Prerequisite to making meaningful measurements in a real combustor environment, however, is the need to develop instrumentation and analytical techniques which will permit the gathering and analysis of experimental data in a very severe environment. Accordingly, the primary effort of the supersonic combustion study reported herein has been directed toward meeting these basic needs. This report describes the work done at APL in the area of H_2-air supersonic combustion over the past two years. Porrions of the work have been previously described in abridged forms, (Refs. 11, 12). Considerable work has been done and is continuing in similar programs supported by the U. S. Air Force (Refs. 4-6).

TECHNIQUES OF ANALYSIS AND DATA REQUIREMENTS

A fairly complete picture of supersonic combustor performance can be developed from knowledge of the absolute and relative magnitudes of heat release and entropy rise or irreversible momentum loss,, Fortunately, over-all measures of these properties can be determined by rather straightforward experimental techniques. The steam calorimeter offers a rather accurate means of measuring over-all heat release, and in the absence of thrust-stand data, pitot-static pressures give meaningful measures of local stream thrust flux which are not very sensitive to the local thermodynamic properties (Ref. 13). Accordingly, it might appear that a more detailed study of the flow field would be unnecessary. However, a detailed picture serves two very important purposes: (1) it permits identification and evaluation of the various mechaniems by which performance is lost (e.g., shocks, poor mixing, incomplete reactions, viscous losses, etc.); (2) it is required in the design and performance evaluation of the nozzle expansion process downstream of the cornbustor exit.

The unique description of combustor performance from experimental results requires complete knowledge of the spatial distributions of pressure, temperature, specie concentrations and velocity in the combustor exit plane. From these properties one can determine any number of defined performance

parameters by comparison with corresponding counterparts that would result in arbitrarily, but meaningfully, defined ideal processes proceeding from the same initial conditions. Moreover, if the combustor air and fuel inlet conditions and the lateral wall transport of mechanical and thermal energy are also known, the identical satisfaction of the integral conservation equations (mass, momentum and energy) and the equations-of-state (thermal and caloric) is assured, The difficulty in using this technique in the analysis of actual combustor tests is caused by the severe instrumentation limitation both in measuring local gas dynamic properties and in determining the temperature and the composition of the gas, which in general contains free radicals. The reverse approach would be to use the integral conservation and the state equations to determine the combustor exit properties; however, this approach requires the simultaneous solution of a set of coupled, integral equations, a near impossible task under normal conditions. A reasonable compromise in this situation is to measure, as well as possible, as many properties as one can and to use the integral equations to determine the others through successive iterations. In practice, even this approach requires compromises due to the nature of the equations and inherent non-uniformity in the flows. Consequently, some simplifying assumptions must be made before the theory can be expeditiously applied. The success of the technique depends upon the reality of the required assumptions and the sensitivity of computed quantities to these assumptions.

Techniques and Requirements

In applying the conservation equations to combustor data analyses, the following assumptions are made: (1) steady-state conditions; (2) axially-directed* velocity at the inlet and exit planes; (3) negligible external forces. Application of the conservation laws to the combustor control volume shown in Fig. 1 results in the following equations:

Mass Conservation:

$$\int_{A_i} \rho_i V_i dA_i + \int_{A_f} \rho_f V_f dA_f = \int_{A_e} \rho_e V_e dA_e \qquad (1)$$

*For conical supply nozzles and combustors, this could easily be modified to a source-flow approximation, of course, if the divergence were significant.

Axial Momentum Conservation:

$$\int_{A_i} p_i dA_i + \int_{A_f} p_f \sin\alpha \, dA_f + \int_{A_w} p_w \sin\alpha \, dA_w - \int_{A_w} \tau_w \cos\alpha \, dA_w - \int_{A_e} p_e dA_e$$

$$= \int_{A_e} \rho_e V_e^2 dA_e - \int_{A_i} \rho_i V_i^2 dA_i - \int_{A_f} \rho_f V_f^2 \cos\beta \, dA_f \qquad (2)$$

Energy Conservation:

$$\int_{A_i} \rho_i \left(h_i + \frac{V_i^2}{2\lambda} \right) V_i dA_i + \int_{A_f} \rho_f \left(h_f + \frac{V_f^2}{2\lambda} \right) V_f dA_f = \int_{A_e} \rho_e \left(h_e + \frac{V_e^2}{2\lambda} \right) V_e dA_e + \dot{Q}_C \qquad (3)$$

It is assumed (and experimentally verified) that the flow is approximately uniform at the combustor and fuel inlet planes. Furthermore, it is assumed that the flow field in the combustor exit plane can be divided into a finite number (n) of concentric areas over which the properties are nearly uniform, implying axisymmetric flow. Under these conditions, Eqs. (1-3) can be integrated to yield, after rearrangement:

Mass Conservation:

$$\rho_i V_i A_i + \rho_f A_f A_f = \sum_{j=1}^{n} \rho_{e_j} V_{e_j} A_{e_j} \qquad (4)$$

Axial Momentum Conservation:

$$p_i A_i + p_f A_f \sin\alpha + \rho_i V_i^2 A_i + \rho_f V_f^2 A_f \cos\beta + \int_{A_w} p_w \sin\alpha \, dA_w$$

$$\int_{A} \tau_w \cos\alpha \, dA_w = \sum_{j=1}^{n} (p_{e_j} + \rho_{e_j} V_{e_j}^2) A_e \qquad (5)$$

Energy Conservation:

$$\rho_i V_i A_i \left(h_i + \frac{V_i^2}{2\lambda} \right) + \rho_f V_f A_f \left(h_f + \frac{V_f^2}{2\lambda} \right) - \dot{Q}_C = \sum_{j=1}^{n} \rho_{e_j} V_{e_j} A_{e_j} \left(h_{e_j} + \frac{V_{e_j}^2}{2\lambda} \right) \qquad (6)$$

The terms on the left-hand sides of Eqs. *(4-6)* are known from experimental measurements and geometry. The term $\int_{A_w} \cos\alpha \, dA_w$ is evaluated by determining a mean value of the wall shear stress from the experimentally measured mean wall heat flux assuming that Reynolds' analogy (Ref. 14) between energy and momentum transport applies. The validity of this assumption is of minor importance since, in our testing, the magnitude of the wall friction force is small compared to other terms in Eq. (5). Examination of these equations reveals that the n-fold unknowns are pressure, p_{e_j}, density, ρ_{e_j}, velocity, V_{e_j}, and enthalpy, h_{e_j}, of the various exit areas, A_{e_j}.

One-Dimensional Analysis

Data requirements and analyses would be relatively simple if the flow in the exit plane were essentially one-dimensional, because (with the input parameters known) the measurement of one exit property (e.g., static pressure) would completely define the remaining unknowns in Eqs. *(4-6)*. In order to determine additional properties in the exit plane such as temperature and entropy, the local gas composition would have to be known. If the chemical species were products of complete combustion (equilibrium composition), the gas composition and temperature would be determined by the fuel-air equivalence ratio and the caloric and thermal equations-of-state:

$$X_{e_k} = X_{e_k}(h_e, p_e, \varphi_e), \text{ and } T_e = T_e(p_e, \rho_e, X_{e_k}), \qquad (7)$$

where X_{e_k} and φ_e are, respectively, the mole fractions of the k chemical species and the equivalence ratio, In the absence of complete combustion, the exact temperature and composition corresponding to the local values of pressure, density and enthalpy would have to be determined from kinetic calculations. However, it is possible to use equilibrium thermodynamic data to define an "effective" equivalence ratio, φ_{eff}, as being that value which with complete combustion would produce the required exit conditions. For $\varphi \leq 1$, this assumption is reasonably good, because the presence of unburned fuel in local equilibrium with the completely burned products does not significantly affect the thermodynamic properties of the mixture, as long as the percentage of dissociated unburned fuel is small. The ratio of φ_{eff} to the value based on measured fuel and air flow rates would provide combustion efficiency. The determined value of entropy rise or stream thrust (i.e., $p_e A_e + \rho_e V_e^2 A_e$) could also be compared with reference values to obtain measures of thrust efficiency. A reasonable model for computing these reference values assumes that heat release equal to the measured value occurs uniformly at a constant area equal to the combustor inlet area in the absence of any heat or viscous losses,

including shocks, followed by isentropic expansion to the combustor exit area. The one-dimensional conservation equations are then used with the known input: conditions and equilibrium thermodynamic data to solve for the reference entropy rise and the quantities with which the reference exit stream thrust is evaluated.

Actual Flow Analysis

In reality, there are significant radial gradients, at least, in the supersonic combustor exit plane. If each flow property distribution can be reasonably approximated by step functions of n steps, then there are *4* n unknowns in Eqs. *(4-6).* The only means of solving this system of equations is to determine by iteration the set of distributions which simultaneously satisfies the equations. This is, obviously, a difficult task, For each property distribution which can be experimentally determined, the solution of the equations becomes more feasible. The measurements which are most conveniently made are cone-static and pitot pressures. Cone-static pressures can be converted to local static pressures p_e, as shown in Appendix C. The local static and pitot pressures can be used with the Rayleigh pitot formula (Ref. 15) to calculate the local Mach number, M_e. The accuracy of this calculation depends upon the specific. heat ratio, γ, used, but in a very weak manner. The momentum flux $\rho_e V_e^2 = \gamma_e p_e M_e^2$, can then be calculated; reasonable techniques, one of which will be described presently, can be devised for estimating γ_e with high accuracy. Thus, cone-static and pitot pressures give the approximate distribution of $\rho_e V_e^2$. Even with these properties established, 3 n unknowns remain in Eqs. *(4-6).* However, $\rho_e V_e^2$ can be used in obtaining an approximate solution of the equations, and, more important, it provides a nearly exact measure of momentum loss or entropy rise.

To proceed with a solution of the equations, some further assumptions are needed concerning the nature of additional properties. In the absence of local temperature measurements, it is assumed that convection is the only mechanism for energy transport throughout the combustor flow field, except in a region or "streamtube" which is identified as the outermost concentric area in the exit plane. In this region the measured heat loss to the wall is permitted. (The validity of this assumption is discussed in the next section.) This assumption permits the integration of the differential energy equation along any path through the combustor, excluding the wall region, the result being a direct relationship between the energy flux at any point in the exit plane and the local relative values of air and fuel mass fluxes. Utilizing the definition of equivalence ratio, $\varphi = (\dot{w}_f/\dot{w}_i)/f_s$, the energy equation can now be written as

$$h_{t_i} - \varphi_{e_j} f_s h_{t_f} - \frac{\dot{Q}_{C_j}}{\dot{w}_{i_j}} = (1 + \varphi_{e_j} f_s) h_{te_j} \qquad (8)$$

where $\dot{Q}_{C_j} = 0$ except for the outermost area, and where $h_t = h + \frac{1}{2} V^2$.

Using the locally measured equivalence ratio with Eq. *(8)* gives local values of $(h_e + \frac{1}{2} V^2)$. The quantity, $\dot{w}_{i_j}$, for the outermost "streamtube" is not known, a priori, and is determined by an iterative process, which can take either of two starting points: (1) the heat loss, Q_{C_j}, can be at first neglected; or (2) the air flow rate, $\dot{w}_{i_j}$, can be taken proportional to the relative size of the "streamtube" exit area.

In the absence of composition measurements, some assumption on the local chemical composition is required before further progress is possible. The approach is to assume a φ_{eff} (as previously defined) and, by an iterative procedure, determine the local h, ρ, and V which satisfy Eq. (8), and the locally measured static and pitot pressures via the real gas, normal-shock relationships (Rayleigh pitot relations). The measured φ distribution determined by gas sampling serves as a bound beyond which the local φ_{eff} cannot exceed. Satisfaction of the momentum and continuity equations and the calorimetrically determined mean φ_{eff} (see Appendix A) is then used as the criterion by which the correct φ_{eff} distribution is established. Since the momentum balance is quite insensitive to φ_{eff}, satisfaction of the other two requirements is the controlling criterion for the analysis, The results of the analysis are used to determine the total exit stream thrust by summation of local values, and to define the mean exit entropy. Performance parameters are then formulated in the manner described for the case of one-dimensional flow. In subsequent discussions, the preceding analysis will be referred to as a streamtube analysis. It is to be noted, however, that no attempt is made to identify lateral boundaries between the inlet plane and a given exit plane sub-area, so use of the word streamtube, which is not strictly applicable in this situation, is based on its descriptive connotation.

This analysis has been programmed on an IBM 7094 computer and centers around the thermodynamic program developed in Ref. 16.

Discussion

The basic assumptions made in the real flow analysis are: (1) thermodynamic properties can be adequately described using equilibrium properties at an "effective" equivalence ratio; (2) convection is the only mechanism of ecergy transport except in the region of the walls, where conduction may also occur. With these assumptions and the available measurements, the conservation equations are solved for all basic flow properties from which performance parameters are deduced. At this point, it is worthwhile to examine the effects of these assumptions on the successful execution of

the analysis and on the accuracy of the deduced properties.

As previously mentioned, assumption (1), though not strictly valid, is reasonably good as long as a negligible amount of unburned fuel is dissociated. .Assumption (2) would be invalid if an appreciable amount of energy were transferred by gas conduction, diffusion or radiation. Except in the wall region, energy transport by the molecular mechanisms is negligible in a supersonic, turbulent flow. However, radiative transport can be significant, but it is small for the test conditions reported herein. For example, consider the radiant energy due to water vapor emission at typical combustor conditions. For an equivalence ratio of 1.0, a static pressure of 1 atm and a static temperature of 5000°F, the partial pressure of water vapor €or complete combustion is 0.26 atm (Ref. 17). Using the emissivity data given in Ref. 18, the energy radiated to the combustor wall is calculated to be ~10 Btu/sec. The experimentally measured combustor heat loss for the same conditions is typically ~ 350 Btu/sec. Assuming complete absorption at the wall, this calculation indicates ~ 3% energy loss due to water vaporradiation. If radiation from other species such as OH, O and NO, all of which are present in only small amounts, is considered, then the radiation loss to the wall is probably less than 5%, even at these ideal conditions. Radiation between gaseous species is much less due to their lower absorptivities.

If either assumption (1) or (2) is invalid in a particular situation, some difficulty will be encountered in satisfying the conservation equations and the experimental measurements exactly. However, the deduced stream thrust, $\mathfrak{F}$, is negligibly affected by local chemical composition and only mildly affected by the local temperature, so that a reasonably good determination of the local temperature is sufficient for this determination. To illustrate this point, the variations of weight flow rate, $\dot{w}$, and $\mathfrak{F}$ with φ, h_t, p_{t_e}, and p_e for typical test conditions are shown in Fig. 2. At h_t = 1361 Btu/lb, the change in $\mathfrak{F}$ for a φ change of 0.2 to 0.9 is only 1.2%, whereas the corresponding change in $\dot{w}$ is 18%. At φ = 0.2, the changes in $\dot{w}$ and $\mathfrak{F}$ due to a 11% change in h_t are 4% and 1%, respectively; at φ = 0.9, these values become 3.2% and 2.1%, respectively. For a constant h_t, a 10% decrease in p_e results in decreases in $\dot{w}$ and $\mathfrak{F}$ of 3.4% and 1.1% at φ = 0.5, respectively, whereas a 10% decrease in pitot pressure results in decreases of 8.3% and 9.7%. These results show that stream thrust is closely related to pitot pressure but relatively insensitive to other properties. Thus, it is apparent that with pitot and static pressure measurements, together with an independent measurement of heat release, one can determine the two most important performance parameters, combustion efficiency and stream thrust efficiency, with sufficient accuracy. Not only can the basic performance parameters be determined from static and pitot pressures and an over-all calorimetric measurement with only rough estimates of other flow properties, but by obtaining an optimum closure on the conservation equations, the best flow field description possible with the available instrumentation can be obtained. Moreover, as will become evident in subsequent sections,

it allows an assessment of possible errors which may occur in obtaining experimental data.

EXPERIMENTAL APPARATUS AND PROCEDURE

Test Facility

Figures 4 and 5 show the experimental arrangement. The combustor is supplied by an 8.5° half-angle conical nozzle to which air (or N_2 for mixing tests) is supplied through an electric arc heater. For the supply nozzle being used in these tests (A_{eff} = 0.83 $in.^2$) and at a constant air weight flow rate of 2.85 lb/sec, the arc heater provides a total enthalpy range of 1400-2000 Btu/lb at total pressures of 425-500 psia; pressures up to 640 psia at 1400 Btu/lb and down to 150 psia at 2000 Btu/lb can be attained by varying weight flow rate.

The 19.4-in.-long water-cooled combustor diverges at a 1.5° half-angle from an inlet diameter of 2.7 in. Adjustment of the cooling water flow rate through the 3/16-in. annular passage permits some control of wall temperature, from ~ 400 - 900°F.. Initial tests were conducted with two other combustors which employed different cooling principles; the first of these was a 12.9-in.-long, uncooled model used in Runs (1) and (2) of Table II) whose inner surface was flame-sprayed with zirconium oxide which was tried with the hope of successfully operating with hot walls; the second model was 19.4-in.-long and cooled by external water sprays which offered the possibility of economical cooling. Neither of these models was sufficiently cooled to withstand the severe combustor environment.

Four fuel injector configurations have been tested: (1) an annular wall slot at a 45° downstream angle to the flow, with an offset area to reduce injection interaction; (2) a flush-mounted, wall injector ring with 8 equally-spaced 0.104-in.-diam. radial holes at 90° to the air flow; (3) an injector identical with (2) except the orifices are inclined 45° downstream to the air flow; and (4) a flush-mounted, wall injector ring with 16 equally-spaced 0.073-in.-diam. holes at 45° to the air flow. Photographs of the injectors are shown in Fig. 5.

The hydrogen heater used in the initial portion of this program consisted of a 300-lb block of nickel 200 into which multiple interconnected flow passages were drilled and capped by welding. The block was heated to ~ 2000°F in a furnace prior to testing. This design proved unsatisfactory, because excessive thermal stresses upon temperature cycling eventually led to cracking, particularly in welded areas.

A better heater, currently in use, has been made from a nickel tube that is resistance-heated (Fig. 6). The 384-in.-long 0.500-in. I.D. x 0.312-in. wall, thermally insulated tube acts as the resistance element in a DC circuit. It is heated to 1000°F in 60 minutes by the 1000-amp battery charger, then it is rapidly heated (5 minutes) to 2000°F by the 10 submarine

[redacted]

battery cells to hold surface oxidation to a minimum. The circuit remains closed during the blowdown phase and supplies 13% of the total power to the gas; 0.07 lb/sec of hydrogen can be delivered at 2200°R and 1000 psia for more than 20 seconds. Figure 7 shows an exit temperature history for a H_2 flow rate of 0.05 lb/sec.

In the process of calibrating the heater, data were obtained on the electrical resistivity (ρ) of the material as a function of temperature (Table I). Between the listed points, the material exhibits a near linear characteristic with the listed slope, α.

Combustor Instrumentation

Typical instrumentation in the combustor exit plane is shown in Fig. 8. The water-cooled pitot pressure and gas sampling probes are made from concentric pairs of tubes in which the water in the outside tube is discharged overboard approximately 3/16 in. downstream of the probe tip. The inner tube of the gas sampling probe has a sharp lip and a 2:1 internal area expansion aimed at providing shock attachment and supersonic expansion that might partially quench reactions within the probe. The 15° half-angle cone-static pressure probes have water-cooled tips made of either copper or tungsten-10% tantalum and have four pressure taps at 90° spacing, each connected to its own transducer. When multiple-hole fuel injectors are used, the probes are located in exit plane positions both in line with and between fuel ports. The remaining combustor instrumentation consists of 38 static pressure taps and 4 thermocouples located in the combustor wall. The wall temperatures are used in conjunction with combustor wall coolant flow rates and temperature rise to obtain the wall heat flux and deduce the wall shearing stress. Motion pictures are also taken of the combustor exit flow field.

The gas samples taken during combustion tests pass through a magnesium perchlorate dessicant for water removal and weight analysis and then into a valved storage container. The equipment (Figs. 9(a) and 9(b)) has provisions for 7 samples. The dessicant containers (plexiglass) are weighed before and after a test. The storage tanks have provisions for pressure and temperature measurements. Prior to acquisition of a commercial gas chromatograph which is now used to analyze for H_2, O_2, and N_2, analysis was made using a thermal conductivity cell for H_2 and an analyzer which detects magnetic susceptibility for O_2 and NO_2-N_2O_4. For N_2-H_2 mixing tests, the unit illustrated in Fig. 9(c) and shown in Fig. 4 is used. This unit consists of 21 storage containers which allows samples to be taken at three different fuel settings during a single run.

The steam calorimeter has a 7.4-in. I.D., a 0.3-in. cooling water passage and is 63.0 in.-long. (A model having an 11.5 in. I.D. had been used in early testing but was replaced because of its excessively long temperature-time response caused by heat losses to the large surface area.)

[redacted]

The wall temperature is operated at -350^{o}F in order to avoid quench water condensation. The bulk of the calorimeter quench water is supplied by the instrumentation probes located at the combustor exit. When necessary, additional water is supplied by spray nozzles (see Fig. 8) 0.5 in. downstream of the probe rakes, The quenched gas temperature is typically 1000^{o}F and is measured by 12 thermocouples located at the exit plane (Fig. 10). Static and total pressures are also measured at the calorimeter exit and used to determine the exhauster pressure level required to maintain a low exit velocity. With the measured wall-cooling rate and quench water injection rate, the combustor bulk heat release is determined.

Test Procedures

Tests normally are of 25-30 sec. duration, Nitrogen is purged through the hydrogen heater prior to arc-heater operation in order to pre-heat the fuel lines and injector to permit rapid establishment of steady-state test conditions. In combustion tests, fuel flow is initiated immediately after arc-heater firing and gas sampling is begun 2 sec. later and continued for 8 sec. After-completion of sampling, two other fuel settings are established and maintained for *6* sec. each, during which time calorimeter data are obtained. Finally, calorimeter data in the absence of fuel injection are obtained. In mixing tests, a similar procedure is followed with gas samples being taken at 3 fuel settings. Thetechniques followed to deduce free stream static pressure from cone probes, equivalence ratio from gas sampling, and heat release from calorimeter measurements are described in the Appendix.

RESULTS AND DISCUSSION

Combustor Inlet Air Profiles and Properties

Figure 13 shows the Mach number profile in the combustor inlet plane deduced from pitot-to-total pressure ratios; in the inviscid portion of the flow, M_1 is within $\pm$ 0.05 of the computed one-dimensional value based on equilibrium isentropic expansion from the arc chamber.

Several methods have been used to determine the temperature gradient in the combustor entry flow field and to verify the mean enthalpy level as deduced from mass flow rate, arc pressure, and effective nozzle throat area. In one of these tests, the temperature at the stagnation point of a hot body was measured by a radiation pyrometer and compared to the computed value based on deduced arc enthalpy. Figure 12 shows the temperature-time history of a 3/8-inch radius pyrolytic graphite probe at two locations in the arc exhaust jet. A direct luminosity photograph is shown in the inset. The measured temperature was $250^{o} \pm 50^{o}$F above the computed value for the centerline position and 150^{o}F + 250^{o}F below the computed value for the 3/4-in. offset position. It appears—that the mass balance method of obtaining arc chamber enthalpy probably yields a reasonable mean (time and volume averaged) value, but a small radial gradient, as well as a fluctuation, is present. In another test, a total temperature probe was tested in arc-heated nitrogen. The tungsten-3% rhenium vs tungsten-25% rhenium thermo-

couple was insulated with beryllium oxide within a tungsten-10% tantalum body. The probe indicated a jet centerline mean total temperature of 5800°R, which compares with 6010°R computed from the mass balance technique. If the 210°R difference is due to probe recovery, then the recovery factor was 94%.

The question of air composition is extremely important in such ground testing of scramjet combustors. Gas samples withdrawn at the combustor inlet showed an O_2 concentration of approximately 19.4 mole percent, based on the assumption that the sample tank contained O_2, N_2 and NO_2-N_2O_4 only (presumably, NO in the sampled gases combined with O_2 to form equilibrium NO_2-N_2O_4 in the tank). This level of O_2 concentration implies an NO concentration of 3.1%, which is equivalent to the equilibrium value at the supply nozzle throat conditions and suggests freezing of the NO at that point. In order to study this feature more closely, a gas sample was withdrawn from the nozzle throat and analyzed specifically for NO_2-N_2O_4 by infrared absorption. This analysis indicated a sample tank concentration of 7.2 mole percent NO_2-N_2O_4 which corresponds to 11.1% NO and 15.4% O_2 in the gas stream. This level of NO is considerably higher than the equilibrium concentration at plenum conditions and cannot be readily explained. However, kinetic calculations suggest that this level of NO concentration would slightly improve the H_2-air reaction.

Slot Injection Combustion Tests

The first series of tests was made with the 45° annular wall slot injector before all of the combustor exit instrumentation became available, so that only qualitative conclusions can be drawn from the data. The combustor inlet conditions and fuel injectant conditions are listed in Table 11. None of these tests produced any significant heat release. In runs 1 and 2, the slot width was 0.067 inch, which would have resulted in sonic injection for ER = 1.0 and $p_f = p_i$. However, for the fuel flows tested, the injection slot was unchoked, M_f = 0.38 and 0.53 for tests 1 and 2, respectively. In runs 3 and 4, a spacer in the injector was removed, and the resulting geometry had a constriction upstream of the injection point, so the injection velocities were supersonic, M~2.27 and 2.44, respectively. The static pressure distribution for run 2 shown in Pig. 13 is typical of all four runs. For comparison, computed pressure distributions are shown for (a) isentropic expansion with no Injection, (b) isentropic expansion of the air and injected H_2 in the absence of mixing and heat release, and (c) instantaneous mixing followed by equilibrium combustion. The mean of the measured pressure distribution more nearly follows case (b). The irregularities in the measured pressure distribution are due to reflected compression shocks and expansion waves. The first compression wave resulted from a change in flow divergence angle of 8.5° at the air supply nozzle to 2.5°, the combustor divergence angle in this test, at the point of fuel injection. To illustrate this point, the pressure rise which would result from the boundary flow at the nozzle exit being turned to its new direction through a plane, oblique shock is shown in Fig. 13. This computed pressure

satisfactorily predicts the combustor inlet wall pressure.

To date there is not an analytical solution available for the mixing, including kinetics, of two streams with different flow directions in a varying pressure field, However, the results for the slot injector have been examined in the following two theoretical models, and in each case ignition would be predicted:

(1) A premixed stream starting at the combustor inlet conditions followed by a constant-pressure reaction and expansion using the kinetic calculations developed in Ref. 19. This analysis suggested an ignition delay distance of less than 2.0 in. Since reactions involving N_2 were not considered in Ref. 19, the technique was modified to include 8 reactions involving the oxides of N_2 in order to determine how large amounts of initial NO would affect the reaction history. As shown in Fig. 14, the induction time is not markedly affected by the presence of NO, but the rate of heat release is increased (compare results at 3.2% NO). Increasing the NO concentration from 3% to 10% caused a further increase in heat release rate, but at 13.5% NO, it fell off somewhat. These results are noticeably different from those obtained in recent shock tube studies of the effect of NO on H_2-air kinetics at low temperatures (below 2000°R) where it was found that even small amounts (1%) of NO substantially reduced the induction time (Ref. 20).

(2) An approximate solution to the mixing of two coaxiai streams in a constant pressure duct (Ref. 21). Realistic initial boundary layer profiles for the fuel and air are assumed and isotherms and concentration profiles are predicted. The kinetics used in Ref. 19 are then roughly superimposed on the flow field to see whether residence times at various temperature levels would suggest ignition.

The subsequent favorable results with discrete-hole injection suggest that no major experimental error existed in the tests and imply that the theoretical models are not adequate descriptions of the actual flow. This is obviously true for the first. model. since it entirely neglects the effect of mixing.

Multiple-Hole Iniection Combustion Tests

Tests with 90°, 8-hole injector. - Combustion has been readily established with the multiple-hole injectors under all test conditions (Table III). Combustor wall pressure distributions measured with the 90°, 8-hole injector are shown in Fig. 14. Pig. 15(a) shows the effect of equivalence ratio at a nearly constant fuel temperature. Also shown in Fig. 15(a) is a typical pressure distribution measured in the absence of fuel injection where the pressure rise at the combustor exit was caused by an excessively high facility exhaust pressure, These measured distributions are to be compared with those expected from one-dimensional, isentropic expansions of air alone and air plus fuel in the absence of mixing

and heat release which are also shown in Fig. 15(a). The measured pressure levels increase with increasing equivalence ratio (φ). The irregularities are due to shocks and expansion waves generated by the initial injection interaction, a flow boundary discontinuity 1.28 in. downstream of the injection plane (see Fig. 3), and reflections of waves from these sources. Comparison of pressures measured 0.15 in. upstream and immediately downstream of the injection station show how the injection interaction (as represented by wall pressure) increased in strength with increasing φ; however, the high initial pressure level in run 8 eventually decayed to a level below that of run 7 at the exit plane, indicating less heat release in run 8, which also agrees with the combustion efficiency results (Table III) determined by a one-dimensional analysis.

The effects of fuel temperature on combustor pressure distribution measured with the 90°, 8-hole injector are shown in Fig. 15(b) for an ER of ~ 0.72 at fuel temperatures of 775°R and 1492°R, and at an ER of ~ 0.49 at 640°R and 1058°R. In each case, preheating increases the strength of the interaction (because injection velocity increases for given φ), and a higher pressure-level is maintained throughout the combustor, indicating improved heat release, as is confirmed by the one-dimensional analyses.

In none of the runs made with the 90°, 8-hole injector were gas sampling, cone pressure or calorimetry data obtained, so that the streamtube analysis previously described could not be rigorously applied, nor could combustion efficiency (η_c) be accurately determined. As previously discussed, η_c can be estimated by a one-dimensional analysis, using wall-static pressure as the only known property in the exit plane. The η_c's so estimated for runs 5-10 in Table III may be inaccurate, but they probably are indicative of the trends that occurred.* The streamtube analysis was attempted on run 10, however, by using the measured pitot pressure distribution, assuming a uniform static pressure equal to wall exit value and determining a distribution of φ_{eff} which approximately satisfied the continuity and momentum equations. The result is presented here because it demonstrates a useful feature of the streamtube analysis, that of indicating which assumptions on the flow field are poor (or which measurements may be in error). The magnitudes of known input and deduced exit quantities pertinent to run 10 are shown below the corresponding terms in Eqs. (4) and (5), in which the numerical quantities are given in lb/sec and lb, respectively:

---

* Some of the combustor inlet conditions and η_c's shown in Table III were reported in Refs. 11 and 12. These previously reported values are in error due to the use of an incorrect supply nozzle discharge coefficient (C_D) in calculating air total enthalpy. Recent calorimetric measurements indicate C_D to be 0.91 (used for data analysis in this report) which is less than the value of 0.985 used for data analysis in Refs. 11 and 12. This surprisingly low C_D is apparently the result of an unusual nozzle design which consists of two conical sections connected by a 1.078-in.-diam. by 1.078-in.-long cylindircal throat (the supply nozzle is actually the throat section of a M-7 wind tunnel). It is also possible that the throat effective area is reduced by swirling motion of the gases (Ref. 29). A definite swirl has been observed with the arc-heated air which results from the purposely induced rotating arc column motion.

$$\rho_i V_i A_i - \rho_f V_f A_f = \sum_j \rho_{e_j} V_{e_j} A_{e_j} \qquad (4)$$

2.86 + 0.041 = 2.858 + 0.043
air "effective" fuel (Discrepancy = 0, forced)

$$(p_i + \rho_i V_i^2) A_i + (p_f \sin\alpha + \rho_f V_f^2 \cos\beta) A_f + \int_{A_w} p_w \sin\alpha \, dA_w - \int_{A_w} \tau_w \cos\alpha \, dA_w$$

(606.3) (0.7) (88.9) - (39.6)

$$= \sum_{j=1}^{10} (p_{e_j} + \rho_{e_j} V_{e_j}^2) A_{e_j} \quad (1b) \qquad (5)$$

(706.2) (Discrepancy = + 7.6%)

The significant features of these results are: (1) the φ_{eff} distribution necessary to satisfy mass continuity was found to be one which accounts for 99.9% of the air mass but requires an excessive amount of fuel, i.e., the results indicate $\eta_c = 1.05$; (2) the deduced exit stream thrust is too high by 7.6%. An $\eta_c < 1$ for this run would require a φ_{eff} distribution which gives a lower fuel flow rate, but Fig. 2 shows that a lower φ_{eff} gives a higher total weight flow rate, so Eq. (4) could not be satisfied. Furthermore, since Fig. 2 shows that the φ_{eff} distribution has a negligible effect on the exit stream thrust, adjusting it would not balance Eq. (5) either. Thus, changes in some other property (or properties) is required in order to obtain a reasonable η_c together with acceptable balances on mass and momentum. Figure 2 shows that, for a constant total weight flow rate, a decrease in φ_{eff} requires either a reduced static or pitot pressure, the latter being more effective. Accordingly, it is concluded that the static pressure, which was assumed uniform at the wall value, and the measured pitot pressure must have been significantly lower in some regions of the flow than the values used in the analysis. Results obtained in a test described in the next section give credence to this conclusion.

Tests with 45°, 8-hole Injector. - Combustor wall pressure distributions measured with the 45°, 8-hole injector are shown in Fig. 15(c). The distribution measured in Run 11 with no injection and the corresponding computed ideal distributions are also shown. Comparison of runs 11 and 12 with runs 6 and 9 for 90° injection in Fig. 15(b) shows that the injection interaction is smaller with partially downstream injection, and the downstream pressure distribution is smoother. A slightly increased pressure level in run 12 due to a higher ER is also noted. The one-dimensional estimates of η_c for runs 6 and 12 in Table III are 70% and 68%, respectively, suggesting that partially downstream injection may not affect η_c appreciably, but

since inlet conditions were somewhat different, this cannot yet be a firm conclusion.

The most complete set of measured combustor exit data obtained to date was taken in run 12 and is shown in Fig. 17, where data points for pitot pressure and static pressure, deduced from cone-static probes, are plotted. Flow striation, characteristic of the 8-discrete-hole injectors results, is apparent from the differences in pitot pressures obtained from probes aligned with and between injection orifices. Figure 19 shows the discoloration patterns (heat streaks) along the combustor wall caused by the striated flow. Calorimetric data for run 12 indicated $\eta_c = 0.56$. (Gas sampling data obtained in this test had to be discarded after it was found that the mild steel sample bottles were causing an appreciable decrease in sample O_2 content prior to analysis,)

The concentric streamtube analysis technique has beer. applied to run 12, using an assumed mean pitot pressure distribution (dashed curve in Fig. 17 between in-line and interdigitated data). An φ_{eff} distribution (Fig, 17) was found which agreed with the calorimetrically measured η_c and more closely satisfied Eqs. (4) and (5). The mean φ distribution necessary for fuel mass conservation was deduced by assuming that a similarly shaped profile held between the mean and "effective distributions. In the energy equation, Eq. (10), the $\dot{Q}_{C_{wall}}$ was measured to be 190 Btu/sec. The magnitudes of the various terms in Eqs. (4) and (5), given in the same order as on 'page 14, were as follows:

$$2.80 + 0.048 = 2.78 + 0.027 \qquad (4)$$

air "effective" fuel

Discrepancy = - 1.4%; 56% of fuel effective.

$$646.2 + 5.8 + 48.5 - 23.4 = 711.0 \qquad \text{Discrepancy} = + 2.0\% \qquad (5)$$

Although a slightly different assumption on the mean pitot pressure distribution shown in Fig. 17 could be made such that the momentum balance would be improved, the above results are considered acceptable. The wall shearing stress term (-23.4, deduced by Reynold's analogy) accounts for only 3.4% of the momentum, hence a 25% error in it would change the magnitude of the left-hand side of Eq. (5) by less than 1%.

The deduced T_e, M_e, w_e and θ_e profiles for run 12 are shown in Fig, 18. With these results and the meastired p_e profile, it is possible to make comparisons of performance with reference cases (e.g., one-dimensional, constant pressure combustion (Ref. 22), and to predict nozzle expansion with certain basic assumptions (Ref. 23).

Obviously, the flow field at the combustor exit plane is far from uniform, and it is not surprising that η_c's computed for one-dimensional flow are often unreasonably high (> 100%). For run 12, a one-dimensional η_c of 68% was computed, which is 21% higher than the 56% measured in the

calorimeter. It cannot be certain that this same difference exists in every test listed in Table III (the difference has to be at least 25% in run 5), however, this result is believed to be indicative of the qualitative differences existing between the true η_c's and the one-dimensional value.

Tests with 45°, 16-Hole Injector. - This injector was designed to eliminate the flow striations noted with the 8-hole injectors. The hole diameter was reduced to 0.073-in., so that total hole area remained the same. Sufficient data are not yet available to determine if this objective was accomplished quantitatively, but heat streaking on the wall was noticeably reduced. Run 13 was conducted with this injector, and the resulting combustor wall pressure distribution is shown in Fig. 16(b). Comparison of Figs. 16(a) and (b) shows similar pressure profiles for run 12 and run 13 for similar fuel conditions. The one-dimensional η_c is ~ 6% lower in run 13, but the higher T_i and p. in run 12 may have been responsible for the increased heat release. No calorimetric data were obtained in run 13, so that further testing is required to assess the effect of number of injection holes on η_c.

CONCLUSIONS

1. The problem of analyzing results from supersonic combustion experiments has been investigated. It is concluded that an adequate description of the flow at the combustor exit can be developed if the following are known:

   a) A complete description of the inlet air and fuel flows.

   b) The axial distributions of combustor wall static pressure and temperature, and the bulk heat flux through the combustor wall (needed to estimate shear stress as well as combustion effieiency).

   c) Local pitot pressures, cone-static pressures, and equivalence ratio in the combustor exit plane.

   d) Over-all heat release (measured by a steam calorimeter).

These measurements are used in conjunction with the integral conservation equations and state equations to completely define the combustor exit flow properties, The instrumentation required to obtain these measurements in the severe combustor exit environment has been developed and successfully used. It should be stressed that this set of measurements is unique only in the sense that it represents the state-of-the-art in instrumentation. The technique of flow evaluation recognizes the instrumentation limitation and then attempts to obtain the best possible description of the flow. The evaluation of local thermodynamic properties and local combustion efficiency could be greatly improved if static temperatures and/or gas compositions could be accurately measured in situ.

[redacted]

2. Experiments were conducted in a conical combustor with an I.D. of 2.7 in., exit/inlet area ratio of 2, and length of 20.5 in. Arc-heated air was supplied at conditions simulating flight at Mach numbers near 8 and altitudes near 113,000 ft. Application of the instrumentation and detail flow analysis (concentric-streamtube) technique has revealed the very non-uniform nature of the combustor exit flow and has shown that one-dimensional flow analysis is inadequate. Any values of η_c for scramjet combustors based on a one-dimensional analysis should be viewed with reservation; although trends, among very similar tests, may be correct, absolute values may be in considerable error. Limited calorimetric data obtained in our tests indicate that the computed one-dimensional η_c's should be reduced by $\sim$ 20%. The streamtube analysis is also useful for assessing experimental data and analytical assumptions.

3. The results have shown a strong effect of injector geometry on the attainment of good supersonic combustion. Annular-slot, low-pressure injection produced insignificant heat release, whereas high-pressure, discrete-hole injection at 45° (downstream) to 90° produced significant combustion [η_c (corrected) $\gtrsim$ *49%)* in all tests. The data show improved combustion efficiency at a given fuel temperature with increasing φ up to the vicinity of stoichiometric proportions (for $T_{tf} \sim 700^\circ R$, η_c increased from *49%* at $\varphi = 0.5$ to 68% at $\varphi = 0.94$), and a highly beneficial effect on combustion efficiency of fuel preheating (η_c near 100% was obtained at $T_{tf} = 1500^\circ R$ for $\varphi = 0.73$).

[redacted]

APPENDIX A: GAS SAMPLING DATA REDUCTION

Equivalence Ratio Determination

In analyzing gas sampling data, it is assumed that for typical test conditions the following scheme represents stages of the H_2-air reaction history:

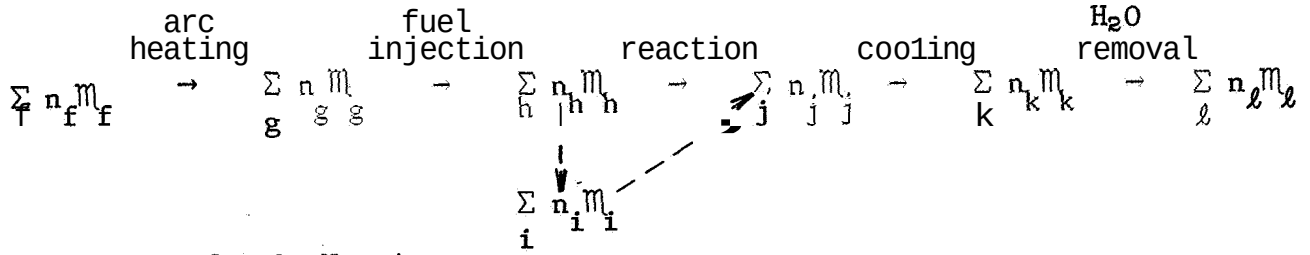

$f = O_2, N_2, A$

$g = O_2, N_2, A, NO$ (A-1)

$h = H_2, O_2, N_2, A, NO$

$i = H_2, O_2, N_2, A$

$j = H_2O, H_2, O_2, N_2, A, H, OH, O, NO, N$

$k = H_2O, H_2, O_2, N_2, A, NO_2, N_2O_4$

$\ell = H_2, O_2, N_2, A, NO_2, N_2O_4$

where it is noted that the conversion of NO to NO_2-N_2O_4 is nearly complete at ambient temperature (Ref. 24). For convenience in defining equivalence ratio, φ, the hypothetical condition i is defined as one in which the species coexist in their basic molecular states as unreacted fuel and unheated air, Analysis of the cooled gases is used to determine φ_i of the combustion products from the definition:

$$\varphi_i = \left[n_{H_2} / (0.463\, n_{O_2} + 0.405\, n_{N_2} + 0.578\, n_A) \right]_i \qquad \text{(A-2)}$$

The molal quantities appearing in Eq. (A-2) are determined from a mass balance applied to the reaction scheme (A-1) which results in the following equations

$$\left(n_{H_2}\right)_i = \left[n_{H_2O} + n_{H_2} + \tfrac{1}{2}\left(n_{OH} + n_H \right) \right]_j = \left(n_{H_2O} + n_{H_2} \right)_k = \left(n_{H_2O} \right)_k + \left(n_{H_2} \right)_\ell \qquad \text{(A-3)}$$

$$\left(n_{O_2}\right)_i = \left[n_{O_2} + \tfrac{1}{2}\left(n_{H_2O} + n_{NO} + n_{OH} \right) \right]_j = \left(\tfrac{1}{2} n_{H_2O} + n_{O_2} + n_{NO_2} + 2\, n_{N_2O_4} \right)_k \qquad \text{(A-4)}$$

$$= \left(\tfrac{1}{2} n_{H_2O} \right)_k + \left(n_{O_2} + n_{NO_2} + 2\, n_{N_2O_4} \right)_\ell$$

$$\left(n_{N_2}\right)_i = \left(n_{N_2} + \tfrac{1}{2} n_N + \tfrac{1}{2} n_{NO} \right)_j = \left(n_{N_2} + \tfrac{1}{2} n_{NO_2} + n_{N_2O_4} \right)_k = \left(n_{N_2} + \tfrac{1}{2} n_{NO_2} + n_{N_2O_4} \right)_\ell \qquad \text{(A-5)}$$

$$\left(n_A\right)_i = \left(n_A\right)_j = \left(n_A\right)_k = \left(n_A\right)_\ell \qquad \text{(A-6)}$$

[redacted]

It is assumed in the definition of φ that combustion has occurred with dry air* of the following volumetric composition, which is also used in calculating equilibrium compositions and thermodynamic properties: 20.950% O_2, 78.088% N_2, and 0.962% A. Since $2NO_2 \rightleftarrows N_2O_4$ is a rapid, reversible reaction, the equilibrium state in the sample bottle can be represented as

$$n_{N_2O_4}/n_{NO_2} \equiv \alpha = \alpha\left(T_g,\ p_{NO_2 + N_2O_4}\right) \tag{A-7}$$

where $p_{NO_2 + N_2O_4}$ is the sum of the partial pressures of NO_2 and N_2O_4. Equilibrium data, such as those given in Ref. 25 are used to determine α as a function of T_g and $p_{NO_2 + N_2O_4}$.

With the aforementioned relationships, it is necessary to determine the mole fractions (partial pressures) of any three of H_2, O_2, N_2 and NO_2, the fourth being inferred as the remaining mole fraction of bottled gases. Water is removed from the sample by magnesium perchlorate before it is bottled. Prior to acquisition of a gas chromatograph, analysis was made for H_2 with a thermal conductivity cell and for O_2 and NO_2 with a paramagnetic analyzer. With the chromatograph, analysis is made for H_2, O_2 and N_2. Depending upon which of N_2 or NO_2 is analyzed, the other can be determined from the equation.

$$\left[1.012\ X_{N_2} = 1 - (X_{H_2} + X_{O_2}) - X_{N_2O_4}\ (1.006 + 1.012\ \alpha)\right]_{\ell} \tag{A-8}$$

where use has been made of the known $\left(n_A : n_{N_2}\right)_i$ ratio. The remaining constituents are given by $X_{N_2O_4} = \alpha\ X_{NO_2}$, and $\left\{X_A = 0.012\left[X_{N_2} + X_{NO_2}\ (\alpha + \tfrac{1}{2})\right]\right\}_{\ell}$.

To determine concentrations prior to water removal, the known $\left[n_{N_2} : n_{O_2}\right]_i$ ratio is used. If we consider one mole of bottled gases, then the corresponding water content in the sampled gases is given by

$$\left(n_{H_2O}\right)_k = \left[0.537\ X_{N_2} - 3.463\ X_{NO_2}\ (\alpha + \tfrac{1}{2})\right]_{\ell} \tag{A-9}$$

With $\left(n_{H_2O}\right)_k$ known, the initial composition n_i, per mole of bottled gases, is now determined from Eqs. (A-3) - (A-6). The results can be used to formulate the following relationship between φ and the measured quantities:

$$\varphi = \frac{X_{N_2} + 1.864\ X_{H_2} - 3.727\ X_{O_2} - 6.455\ X_{NO_2}\ (\alpha + \tfrac{1}{2})}{X_{N_2} + X_{NO_2}\ (\alpha + \tfrac{1}{2})} \tag{A-10}$$

---

* The air, which is saturated at 3000 psi before passing through a process dryer consisting of a molecular sieve dessicant, contains ~ 0.01% water by weight.

[redacted]

The water content of the sampled gases is determined by weight analysis and used as a check on the accuracy of the foregoing analysis. The temperature and pressure of the bottled gases is measured and the volume of the bottle is known, so that the total number of moles of bottled gases is $p_b V_b / RT_b$, and the corresponding weight of water is

$$\left(w_{H_2O}\right)_k = \left(n_{H_2O}\right)_k \mathcal{M}_{H_2O}\, p_b V_b / RT_b \qquad \text{(A-11)}$$

where $\left(n_{H_2O}\right)_k$ is given by Eq. (A-9). This weight of water is compared with that determined from the actual. weight analysis. Assuming the water weight analysis to be accurate, any difference between the measured and computed water contents can be traced to one or both of two possible causes: (1) mass diffusion in the combustor flow field caused by concentration gradients resulting from the chemical reaction, so that local values of the ratio $\left(n_{O_2} : n_{N_2}\right)_i$, in particular, may be different from that existing in pure air; (2) mass diffusion (e.g., H_2 separation) due to flow disturbances created by the sampling probe, particularly if the probe does not swallow the shock. A mass balance over the combustor exit plane determines which of the two mechanisms occur. If only the first mechanism occurs, a mass balance of the hydrogen is possible; if the second mechanism occurs, a mass balance is not possible.

Combustion Efficiencv Determination

In order to determine combustion efficiency from gas sampling data, it is necessary that the sampling probe efficiently quench chemical reactions at the sampling point. Since this has not been proven to occur with our probes, a more accurate means of determining combustion efficiency, i.e., steam calorimetry (see next section), is used. However, the sampling data is analyzed to determine its usefulness for this purpose.

Among the results of the combustor exit flow analysis described in the text were the local φ_{eff}, T_e, and p_e and the corresponding equilibrium composition. With this information, a realistic local composition at the combustor exit or sampling probe inlet is determined as being the equilibrium composition corresponding to φ_{eff} plus unburned fuel in an amount determined by the difference between φ_{eff} and the actual φ. Assuming that no further chemical reaction occurs, except as required by the quenching process, and postulating recombination paths of the active species (O, N, H, OH and NO), the corresponding composition of the quenched sample is calculated. The active specie recombination paths used are as follows: If $\left(n_H > n_{OH}\right)_j$,

$$\sum_j n_j \mathcal{M}_j \rightarrow \left\{\left[n_{OH}\mathcal{M}_{H_2O} + \tfrac{1}{2}\left(n_H - n_{OH}\right)\mathcal{M}_{H_2} + \tfrac{1}{2}\left(n_O - n_{NO}\right)\mathcal{M}_{O_2} + \tfrac{1}{2} n_N \mathcal{M}_{N_2} + n_{NO}\mathcal{M}_{NO_2}\right]_j\right\}_k$$

$$j = OH,\ H,\ O,\ N,\ NO \qquad \text{(A-12)}$$

[redacted]

If $\left(n_H < n_{OH}\right)_j$,

$$\sum_j n_j m_j \rightarrow \left[\tfrac{1}{2}\left(n_H + n_{OH}\right)m_{H_2O} + \tfrac{1}{4}\left(n_{OH} - n_H + 2\,n_O - 2\,n_{NO}\right)m_{O_2} + \tfrac{1}{2}\,n_N m_{N_2} + n_{NO} m_{NO_2}\right]_j$$

$$j = OH,\ H,\ O,\ N,\ NO \qquad \text{(A-13)}$$

It is assumed in deriving Eqs. (A-12) and (A-13) that the maximum amount of water is formed from OH, H and O. If the coefficient of O_2 in the equations is negative, then no O_2 is formed and the amount of O_2 existing at condition (j) must be reduced by the magnitude of the coefficients.

The composition calculated by the above analysis is compared with the actual composition determined from sampling, whereby the quenching efficiency of the sampling probe is assessed. It is important to note that even if the probe completely quenched the sample it is still necessary to perform the above analysis in order to compute combustion efficiency, since the state of the-quenched gases depends heavily upon the state of the hot combustion products. It is not sufficient to use only the amount of fuel in the quenched gases as a measure of combustion efficiency. As an illustration of this point, we note that if the equilibrium composition (i.e., 100% combustion efficiency) corresponding to $\varphi = 1.0$ and 1 atm (Ref. 17) is quenched via the proposed paths from 5500°R to room temperature, 7.8% H_2 will be present which implies 92.2% combustion efficiency based on unburned fuel. This difference is significant.

[redacted]

APPENDIX B: CALORIMETER DATA REDUCTION

Definition of Experimental Heat Release Rate and Combustion Efficiency

To simplify the discussion, it is assumed that average values of the combustor exit flow properties can be defined; generalization to the case where gradients exist is straightforward, but much more complicated. Application of the energy conservation law to the combustor flow (Fig. B-1) results in the following equation:

$$\dot{w}_a\left(h_{t_a}\right)_1 + \dot{w}_f\left(h_{t_f}\right)_2 = \left(\dot{w}_a + \dot{w}_f\right)\left(h_{t_{cp}}\right)_3 + \dot{Q}_C \tag{B-1}$$

where $h \equiv h + \frac{1}{2} V^2 = (H + \Delta H) + \frac{1}{2} V^2$, where h is the static enthalpy at temperature T, ΔH is the heat of formation at an arbitrary reference, T_o, and $H \equiv \int_{T_o}^{T} c_p dT$. The subscripts a, f, and cp refer to air, fuel, and combustion products. If we define sensible enthalpy as $\Delta H \equiv H + \frac{1}{2} V^2$, then Eq. (B-1) can be written as

$$\dot{w}_a\left(\Delta H_a\right)_1 + \dot{w}_f\left(\Delta H_f\right)_2 - \left(\dot{w}_a + \dot{w}_f\right)\left(\Delta H_{cp}\right)_3 = \left(\dot{w}_a + \dot{w}_f\right)\left(\Delta h_{cp}\right)_3 - \dot{w}_a\left(\Delta h_a\right)_1 - \dot{w}_f\left(\Delta h_f\right)_2 + \dot{Q}_C \tag{B-2}$$

The left-hand side of Eq. (B-2) is identified as the heat release rate, $\dot{Q}_R$, i.e.,

$$\dot{Q}_R \equiv \dot{w}_a\left(\Delta H_a\right)_1 + \dot{w}_f\left(\Delta H_f\right)_2 - \left(\dot{w}_a + \dot{w}_f\right)\left(\Delta H_{cp}\right)_3 \tag{B-3}$$

$$= \left(\dot{w}a + \dot{w}f\right)(\Delta hcp)3 - \dot{w}_a\left(\Delta h_a\right)_1 - \dot{w}_f\left(\Delta h_f\right)_2 + \dot{Q}_C \tag{B-4}$$

(Note that this definition of $\dot{Q}_R$ differs from a commonly used definition which requires the reactants and combustion products to be at ambient conditions.)

Combustion efficiency can be defined in either of two ways: (1) the ideal fuel flow rate, $\dot{w}_{f,ideal}$, required to produce the experimental $\dot{Q}_R$ can be divided by the experimental fuel flow rate, $\dot{w}_f$; or (2) the experimental $\dot{Q}_R$ can be divided by the maximum $\dot{Q}_R$ which could be ideally obtained with the experimental $\dot{w}_f$. Since $\dot{Q}_R$ is not a linear function of $\dot{w}_f$, these two definitions differ. The first definition is used in the work reported herein because of its usefulness in engine performance calculations.

To determine the experimental $\dot{Q}_R$, Eq, (B-3) indicates that one should determine the gas composition at various stations in the combustor. However, sampling of the hot combustion products is a difficult task. An alternative, as shown by Eq. (B-4), would be to measure the sensible heats of the reactants and products. In theory, this could be accomplished in the absence of composition measurements if a frozen total temperature could be measured, for then the composition could be determined by an iterative process such that Eqs. (B-3) and (B-4) produced the same value of $\dot{Q}_R$. This approach is further simplified by the fact that at temperature levels of interest the sensible heat is rather insensitive t.o composition, because the majority of the species present have nearly the same specific heats. Nevertheless, this approach is difficult due to the lack of techniques for measuring high temperatures, The steam calorimeter offers a way out of this situation.

Steam Calorimeter

An energy balance of the calorimeter flow (Fig. B-1) results in the following equation:

$$\dot{w}_{cp}\left(h_{t_{cp}}\right)_3 + \dot{w}_w\left(h_{t_w}\right)_4 = \dot{w}_{cp}\left(h_{t_{cp}}\right)_5 + \dot{w}_w\left(h_{t_w}\right)_5 + \dot{Q}_K \qquad \text{(B-5)}$$

If sensible heats and heats of formation are introduced into Eq. (B-5), and the result then introduced into Eq. (B-4), the following equation results:

$$\dot{Q}_R = \dot{w}_{cp}\left(\Delta h_{cp}\right)_5 + \dot{w}_{cp}\left[\left(\Delta H_{cp}\right)_5 - \left(\Delta H_{cp}\right)\right]_3 + \dot{Q}_C + \dot{Q}_K + \dot{Q}_q - \dot{w}_a\left(\Delta h_a\right)_1 - \dot{w}_f\left(\Delta h_f\right)_2 , \qquad \text{(B-6)}$$

where $\dot{Q}_q \equiv \dot{w}_w\left[\left(h_{t_w}\right)_5 - \left(h_{t_w}\right)_4\right]$, and $\dot{w}_{cp} \equiv \dot{w}_a + \dot{w}_f$. The temperature level at the calorimeter exit is relatively low and the velocity is subsonic, so that gas sampling and temperatures can be measured accurately and $\left(\Delta h_{cp}\right)_5$ and $\left(\Delta H_{cp}\right)_5$ can be evaluated. Since the calorimeter quenches the chemical reaction at the combustor exit, the term $\left(\Delta H_{cp}\right)_5 - \left(\quad\right)_3$, would be identically zero were it not for the fact that free radicals existing at station (3) recombine in the quenching process; the result is that this term is significant, Hence, the need to know the Composition of the hot combustion products apparently remains. An alternative approach which avoids any sampling and which is used for data analysis will now be described.

Inasmuch as the calculation of combustion efficiency requires that the $\dot{w}_{f,ideal}$ which would produce the experimental heat release be known, it is reasonable to make use of the composition resulting from this ideal calculation in computing $\dot{Q}_R$. As was previously noted, the sensible heat is relatively insensitive to the composition used in its calculation, so that a reasonably accurate determination of $\left[\left(\Delta H_{cp}\right)_5 - \left(\Delta H_{cp}\right)_3\right]$ will result in an acceptable value for Q_R. Hence the composition used for evaluating Q_R is taken at station (3) as the equilibrium composition corresponding to plus unburned fuel in the amount $\left(\dot{w}_f - \dot{w}_{f,ideal}\right)$. The composition at station

(5) is that which results from quenching the composition at (3) with no change in concentrations of the stable species except as required by the quenching process, where it is assumed that the radical recombination paths are as given in Eqs. (A-12) and (A-13). The problem now reduces to one of determining $\dot{w}_{f,ideal}$ and the composition at station (3).

Calculation of $\dot{w}_{f,ideal}$

The problem of determining $\dot{w}_{f,ideal}$ and the corresponding equilibruim composition is primarily one of defining the ideal static temperature and pressure at the combustor exit; the effect of the flow velocity on these conditions is significant and must be taken into consideration. The mass, momentum and energy conservation laws are applied to this problem under the following conditions: (1) the exit flow is uniform (one-dimensional); and (2) the experimental combustor heat loss and wall pressure force, and the deduced wall frictional force are employed. Under these conditions (and with known input conditions), all of the combustor exit properties corresponding to a given $\dot{w}_{f,ideal}$ can be calculated using equilibrium thermodynamic data. The correct $\dot{w}_{f,ideal}$ is that value which allows simultaneous satisfaction of Eqs. (B-3) and (B-6), and is found by an iterative procedure.

The effects of pressure, temperature (and velocity) and quenching path on calculated heat release rate is shown in the following example. Instead of calculating heat release rate, an equivalent approach in arriving at combustion efficiency is to determine the amount of fuel which, when burned to completion and quenched to the temperature at station (5), would give the measured $(\dot{Q}_q + \dot{Q}_C + \dot{Q}_K)$. If Eqs. (B-1) and (B-5) are combined, we obtain

$$Q_H \equiv \frac{\left(\dot{Q}_q + \dot{Q}_C + \dot{Q}_K\right)}{\dot{w}_{cp}} = \frac{\dot{w}_a}{\dot{w}_{cp}} \left(h_{t_a}\right)_1 + \frac{\dot{w}_f}{\dot{w}_{cp}} \left(h_{t_f}\right)_2 - \left(h_{t_{cp}}\right)_5 \qquad \text{(B-7)}$$

For given air and fuel input conditions and a given temperature at station (5), Q_H will depend only on the composition at (5) which, in turn, depends on the composition at (3) and the quenching path. In Fig. B-2, we show the variation in the term Q_H when the equilibrium combustion products corresponding to $\phi = 1.0$ at 0.5, 1.0 and 2.0 atm (Ref. 17) are quenched via the paths of Eqs. (A-12) and (A-13) from various velocity (or temperature, which is also plotted) levels. For the example shown, it is assumed that

$$\frac{\dot{w}_a}{\dot{w}_{cp}} \left(h_{t_a}\right)_1 + \frac{\dot{w}_f}{\dot{w}_{cp}} \left(h_{t_f}\right)_2 = \left(h_{t_{cp}}\right)_6 = 1942 \text{ Btu/lb},$$

$T_5 = 1440^{\circ}R$ and the kinetic energy at station (5) is negligible. It is also noted in Fig. B-2 that the value of Q_H corresponding to equilibrium cooling of the combustion products (which would be computed using the fuel's higher heating value with a correction to account for the products being at $1440^{\circ}R$ rather than room temperature) is 2945 Btu/lb. As shown in Fig. B-2, pressure has only a minor effect (1% at 7000 fps) on Q_H. However, Q_H increases by 6.5% as the velocity increases from 0 to 7000 fps at 1 atm, This velocity increase corresponds to a temperature decrease of $5700^{\circ}R$ to $5135^{\circ}R$. Even more significant is the difference between the Q_H calculated by assuming quenching and that calculated assuming equilibrium cooling (9.2% at 7000 fps, increasing as the velocity is decreased). These results indicate that reasonably good estimates of temperature and quenching mechanism are important in defining combustion efficiency by calorimetry.

Determination of Air Inlet Enthalpy

It has been assumed in the previous discussion that the air and fuel inlet conditions are known. The highest temperature level at which H_2 is used in tests is $2300^{\circ}R$; hence, temperature measurements are possible. The total temperature of the air, however, is in the range (5000°-$5500^{\circ}R$) where direct measurement is difficult. The calorimeter offers one means of conveniently determining the air total enthalpy. Application of the energy conservation law to the combustor-calorimeter combination in the absence of fuel injection results in the following equation:

$$\dot{w}_a\left[\left(\Delta h_a\right)_1 + \left(\Delta H_a\right)_1\right] = \dot{w}_a\left[\left(\Delta h_a\right)_5 + \left(\Delta H_a\right)_5\right] + \dot{Q}_C + \dot{Q}_K + \dot{Q}_q \qquad \text{(B-9)}$$

The air static temperature at the combustor inlet for the tests reported herein is in the range of 2000°-$2500^{\circ}R$ at a pressure level of $\sim$ 1 atm. If the air were in equilibrium, $\left(\Delta H_a\right)_1$ and $\left(\Delta H_a\right)$ would be zero since only O_2, N_2 and A, all of which have zero heats of formation, would exist (Ref. 17) (actually, a negligible amount of NO would be present). Since a significant amount of NO was found to exist at the combustor inlet, these terms become $\left(\Delta H_a\right)_1 = \left(Y_{NO}\ \Delta H_{NO}\right)_1$, $\left(\Delta H_a\right)_5 = \left(Y_{NO_2}\ \Delta H_{NO_2}\right)_5$ where $\left(Y_{NO}\right)_1$ and $\left(Y_{NO_2}\right)_5$ were found to be 0.032 and 0.046, respectively. Calculation of $\left(\Delta h_a\right)_5$ from the known composition (assumed the same as at station (1)) and the measured temperature now permits $h_{t_a}\big)_1 = \left(\Delta h_a\right)_1 + \left(\Delta H_a\right)_1$ to be determined.

APPENDIX C: CONE STATIC PRESSURE DATA REDUCTION

The determination of free stream static pressure from cone surface pressure measurements can be based on exact conical flow properties such as those presented in Ref. 26. For computational convenience, the analytic approximation of the exact results which is presented in Ref. 27 is used in this program. Even though these results strictly apply only to unyawed cones, they can be used where small yaw angles occur provided the average cone surface pressure is measured (Ref. 28).

The approximation presented in Ref. 27 is

$$C_p \equiv \frac{p_s - p_\infty}{q_\infty} = \tfrac{1}{2}\left(f_2 + f_1 \sin 2\delta - \left\{(f_2 - f_1 \sin 2\delta)^2 - [(f_3 - f_1)\sin 2\delta]^2\right\}^{\frac{1}{2}}\right) \qquad \text{(C-1)}$$

where $f_1 = \frac{\gamma + 7}{4} - \left(\frac{\gamma - 1}{4}\right)^2 + \frac{6}{M_\infty^6} + \frac{M_\infty^2 - 1}{M_\infty^4 \sin\delta}$,

$$f_2 = \tfrac{1}{2}\left(\frac{\gamma + 7}{\gamma + 1}\right)\left(1 - \frac{1}{M_\infty^2}\right)\left(1 + \frac{1}{M_\infty^6}\right)$$

$$f_3 = \frac{\gamma}{2}\left(\frac{\gamma + 7}{\gamma + 1}\right)\left(1 + \frac{1}{M_\infty^2}\right)\left(1 + \frac{1}{M_\infty^6}\right)$$

Application of Eq. (C-1) requires that the local Mach number and specific heat ratio be known. As is shown in Ref. 27, the pressure coefficient, C_p, is only weakly dependent upon γ, so that a value of 1.4 is used in preliminary calculations. The measured combustor exit wall static pressure is used together with the measured local pitot pressure, p_t', to estimate M_∞ (via the Rayleigh pitot formula), which is then used to calculate p_∞ from Eq. (C-1). The process is repeated using p_∞ and p_t' to obtain a new M_∞ until satisfactory convergence is obtained. The value of p_∞ obtained in this manner is used in the analysis described in the text which utilizes real gas properties, so that a final recomputation of p_∞ is made to correct for real gas effects.

[redacted]

REFERENCES

1. G. L. Dugger, F. S. Billig, and W. H. Avery, "Hypersonic Propulsion Studies at the Applied Physics Laboratory, The Johns Hopkins University," (U), Presented at the Ramjet Technical Session of the Joint IAS/ARS Summer Meeting, Los Angeles, Calif., June 14, 1961, APL/JHU, TG 405 (Confidential).

2. W. H. Avery and G. L. Dugger, "Hypersonic Airbreathing Propulsion," Astronautics and Aeronautics, Vol. 2, No. 6, June 1964, pp. 42-47 (U).

3. J. Swithenbank, "Theoretical Performance of Hypersonic Ramjets with Supersonic Combustion," Report No. SCS 25, (U), McGill University, Montreal, Canada, August 1960.

4. "Analytical and Experimental Evaluation of the Supersonic Combustion Ramjet" (U) General Applied Science Laboratories, Inc., APL TDR-64-68 (Confidential), May 1964.

5. "Advanced Air-Breathing Engines Vol. II: Experimental Investigation" (U) General Electric Company, APL TDR-64-21, (Confidential), May 1964.

6. "Applied Research and Advanced Technology of the Supersonic Combustion Ramjet Engine for 1963" (U), Marquardt Corporation APL-TDR-64-44 (SECRET), July 1964..

7. A. Ferri, P. A. Libby, and V. Zakkay, "Theoretical and Experimental Investigation of Supersonic Combustion," (U), Third International Congress, ICAS, Stockholm, Sweden, August 1962.

8. J. A. Schetz, "The Diffusion and Combustion of Slot Injected Gaseous Hydrogen in a Hot Supersonic Air Stream," (U), 35th Bumblebee Design Panel Meeting held at the McDonnell Aircraft Co., St. Louis, Mo., November 20-21, 1963, APL/JHU TG 60-35 (Confidential).

9. A. Vranos, "Supersonic Mixing of Helium and Air," (U), Minutes of the 31st Bumblebee Propulsion Panel Meeting held at The Applied Physics Laboratory, The Johns Bopkins University, Howard County, Md., May 19-20, 1964, APL/JHU TG 63-53 (Confidential).

10. J. H. Morgenthaler, "Supersonic Mixing of Hydrogen and Air," University of Maryland PhD Thesis, May 1.965.

11. C. L. Yates and F. S. Billig, "Supersonic Combustion (Hydrogen)," (U), Aeronautics Division Quarterly Report, (Confidential).

    (a) Section V/24a, APL/JHU SR/7-4, December 1963.
    (b) Section V/22c, APL/JHU SR/7-6, July 1964.
    (c) Section V11/b, APL/JHU AWR/64-3, October 1964.
    (d) Section V11/2a, APL/JHU AWR/64-4, October-December 1964.
    (e) Section V11/2a, APL/JHU AQR/65-1, January-March 1965.
    (f) Section V11/1, APL/JHU AWR/65-2, April.-June 1965.

[redacted]

12. F. S. Billig and C. L. Yates, "Experimental Results and Techniques for Data Analysis of a Hydrogen-Fueled Supersonic Combustor," (U), Talk presented at the AIAA Propulsion Joint Specialist Conference, Colorado Springs, Colorado, (Confidential), June 14-18, 1965.

13. F. S. Billig, "A Study of Combustion in Supersonic Streams," University of Maryland PhD Thesis, May 1964, also APL/JHU BB 321, (U), July 1964.

14. H. Schlichting, Boundary Layer Theory, Fourth Edition, McGraw-Hill Co., New York, 1962.

15. A. H. Shapiro, The Dynamics and Thermodynamics of Compressible Flow, Vol. I, The Ronald Press Co., New York, 1953.

16. D. R. Cruise, "Notes on the Rapid Computation of Chemical Equilibria," J. Physical Chemistry, Vol. 68, No. 12, pp 3797-3802, December 1964.

17. W. C. Brown and D. L. Warlich, "Properties of Combustion Gases. System: H_2-Air," (U), General Electric Co., R62FPD-366 (U) November 1962.

18. M. Jakob, Heat Transfer, Vol. II, John Wiley and Sons, New York, 1957.

19. A. A. Westenberg, "Hydrogen-Air Chemical Kinetic Calculations in Supersonic Flow," APL/JHU CM-1028 (U), December 1962.

20. A. D. Snyder, J. Robertson, D. L. Zanders, G. B. Skinner, "Shock Tube Studies of Fuel-Air Ignition Characteristics," Prepared by Monsanto Chemical Corp., Dayton, Ohio for Air Force Systems Command, AFAPL-TR-65-93, (U), August 1965.

21. J. A. Schetz and S. Favin, "The Ignition of Slot-Injected Gaseous Hydrogen in a Supersonic Air Stream" (U), NASA CR-344 (Confidential), Prepared under Contract No. NOw 62-0604-c with the Bureau of Naval Weapons by the Applied Physics Laboratory, Johns Hopkins University, Silver Spring, Maryland.

22. F. S. Billig, S. E. Grenleski, "Combustor Development for a Liquid-Fueled Supersonic Combustion Missile," (U), Talk presented at the AIAA Propulsion Specialist Conference, Colorado Springs, Colorado, (Confidential), June 14-18, 1965.

23. W. C. Colley and A. Lingen, "Supersonic Combustor Performance Criteria," (U) Minutes of 31st Meeting of the Bumblebee Propulsion Panel, (Confidential), APL/JHU TG-63-53, June 1964.

24. D. M. Post and H. Russel, Jr., Systematic Inorganic Chemistry, Prentice-Hall, New York, 1946, Chap. 1.

25. "Titan II Storable Propellant Handbook (Revision A)," Bell Aerosystems Co., Bell Report 8182-933004, (U), March 1962.

26. "Equations, Tables, and Charts for Compressible Flow," (U), Ames Research Staff, NACA Rept. 1135, 1953.

27. W. E. Simon and L. A. Walter, "Approximations for Supersonic Flow over Cones," AIAA Journal, Vol. I, No. 7, 1963, pp 1696-1698.

28. F. J. Centolanzi, "Characteristics of a 40^{o} Cone for Measuring Mach Number, Total Pressure and Flow Angles at Supersonic Speeds," (U), NACA TN 3967, May 1957.

29. A Mager, "Approximate Solution of Isentropic Swirling Flow Through a Nozzle," ARS Journal, Vol. 31, No. 8, pp 1140-1148, August 1961.

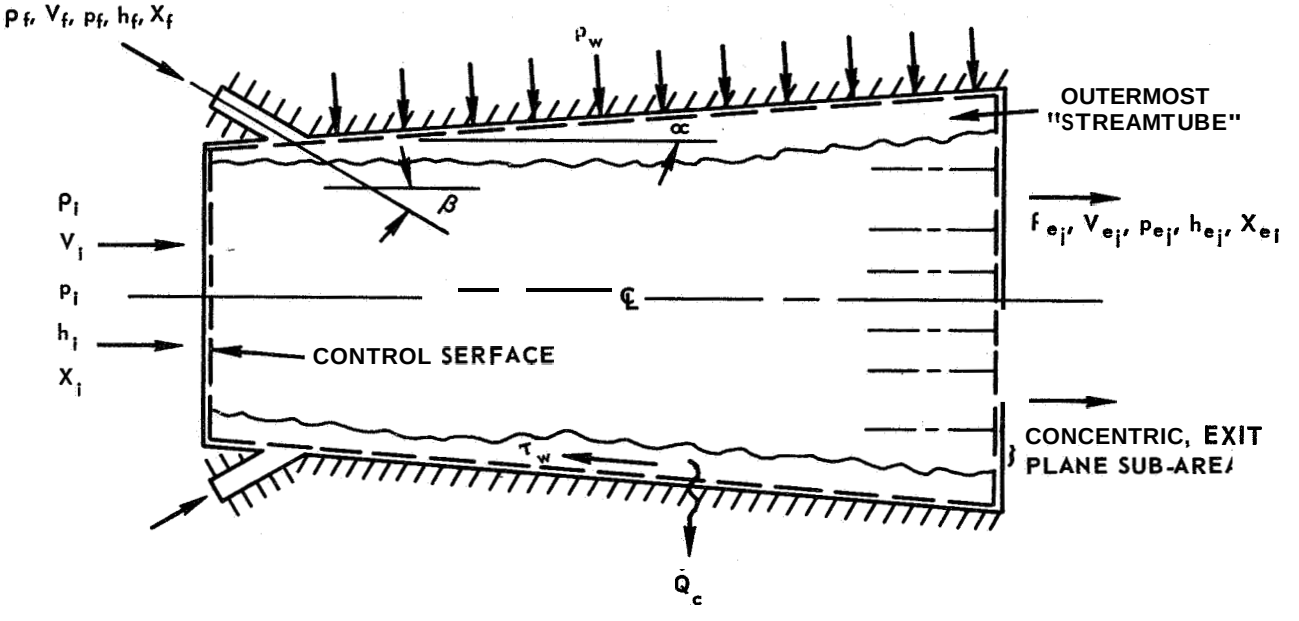

Fig. 1 SUPERSONIC COMBUSTOR ANALYTICAL MODEL

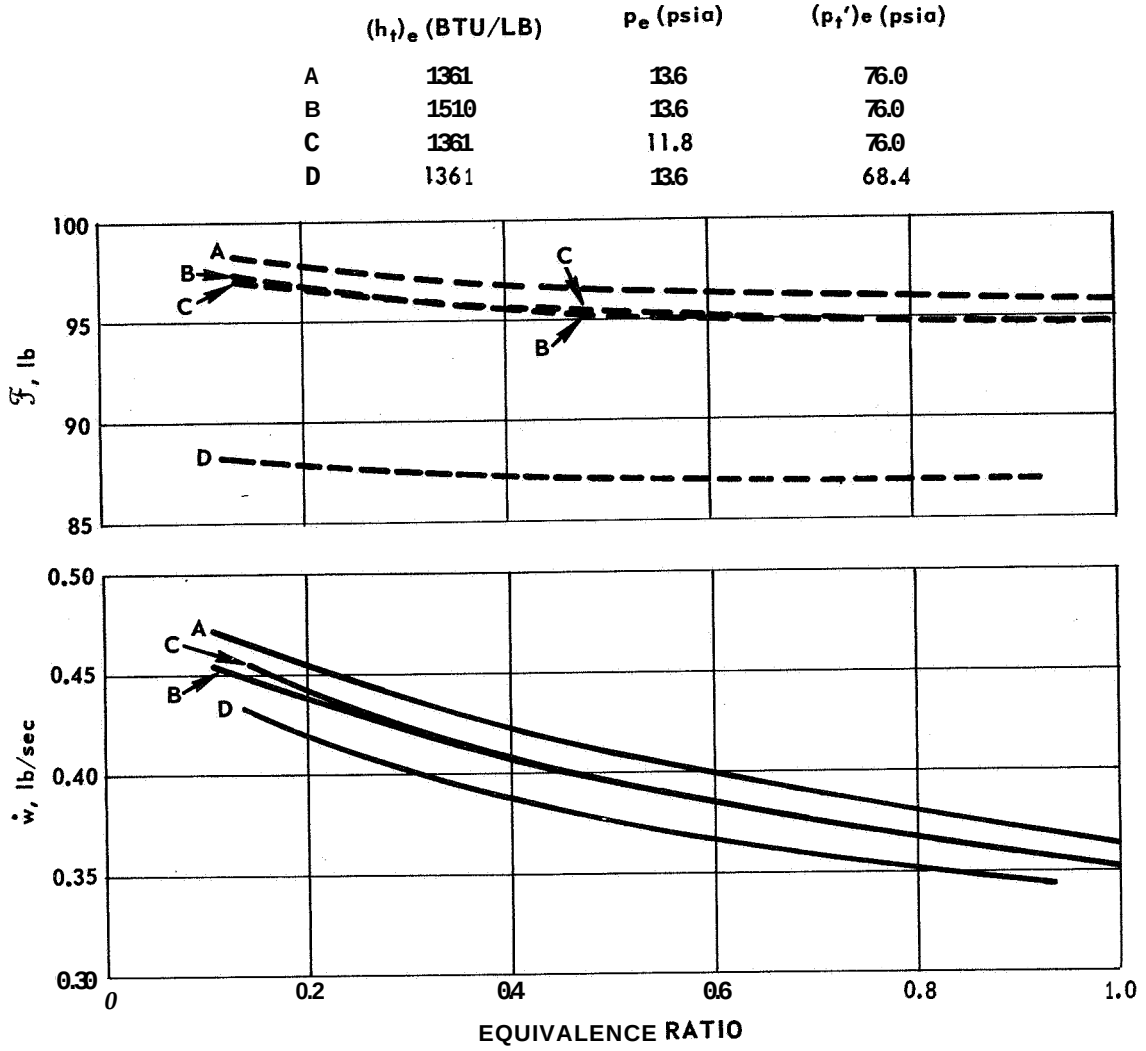

Fig. 2 EFFECTS OF EQUIVALENCE RATIO, TOTAL ENTHALPY, PITOT PRESSURE AND STATIC PRESSURE ON DEDUCED COMBUSTOR EXIT PARAMETERS

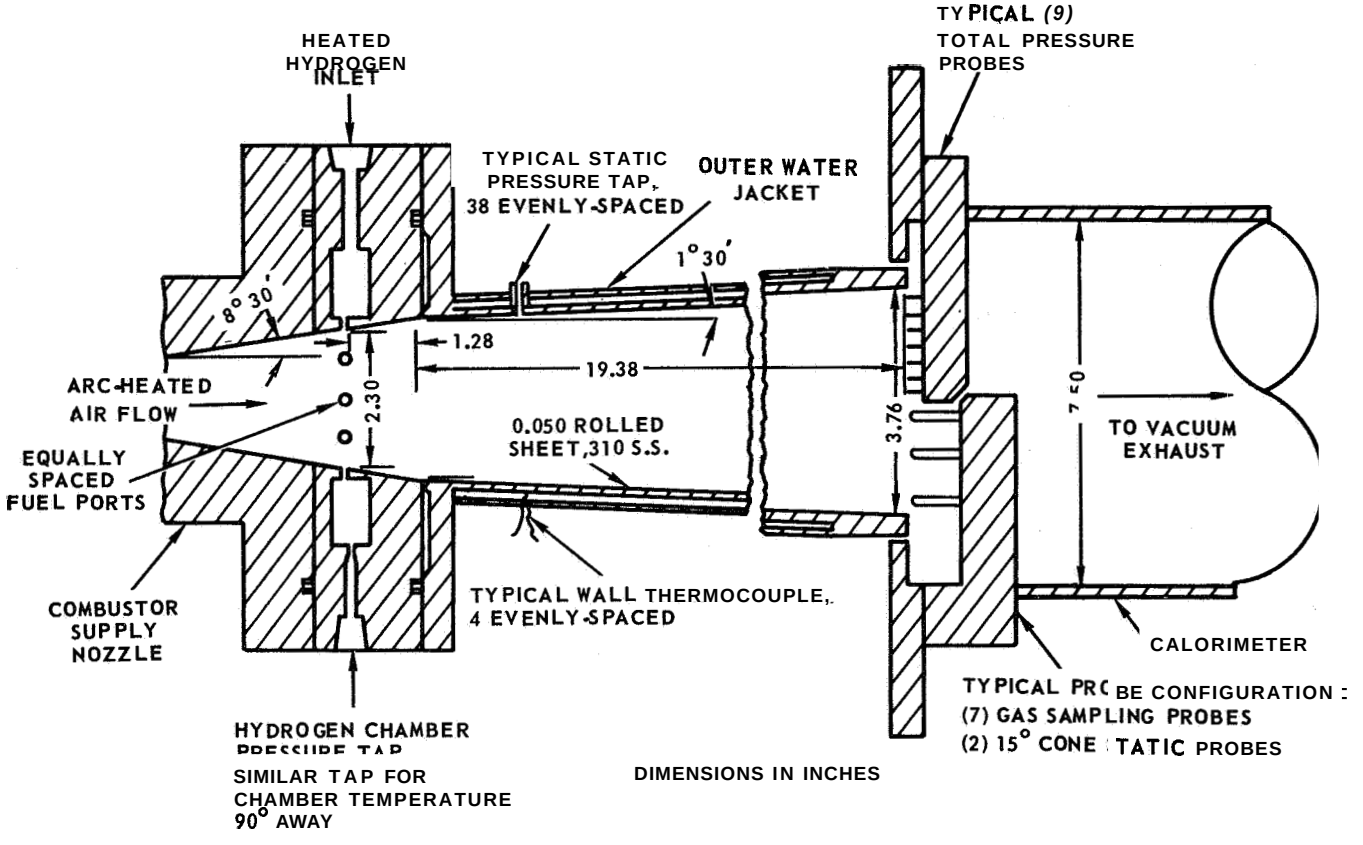

Fig. 3 SCHEMATIC OF COMBUSTOR TEST ARRANGEMENT

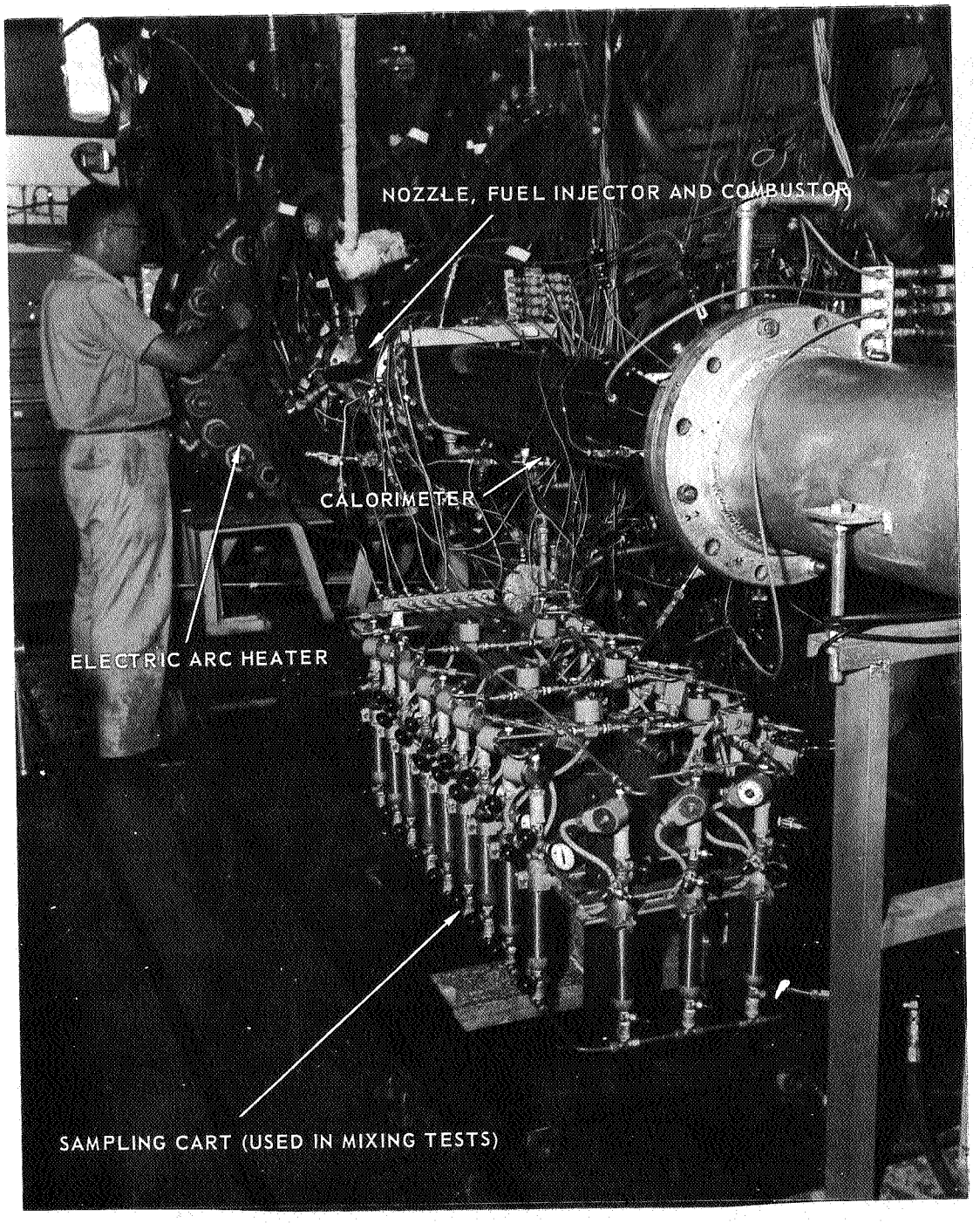

Fig. 4 SUPERSONIC COMBUSTION TEST APPARATUS

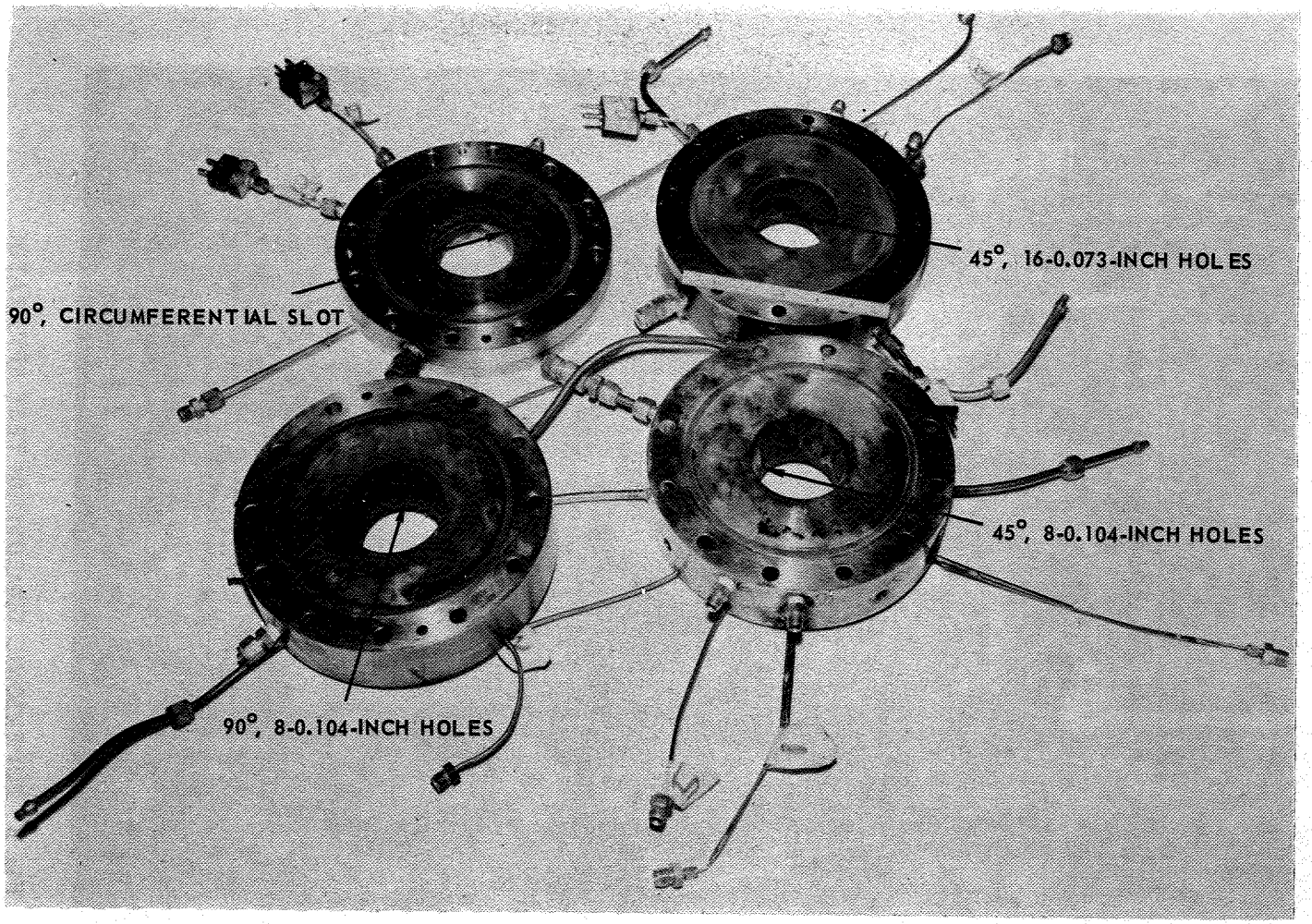

Fig. 5 FUEL INJECTORS USED IN TESTS

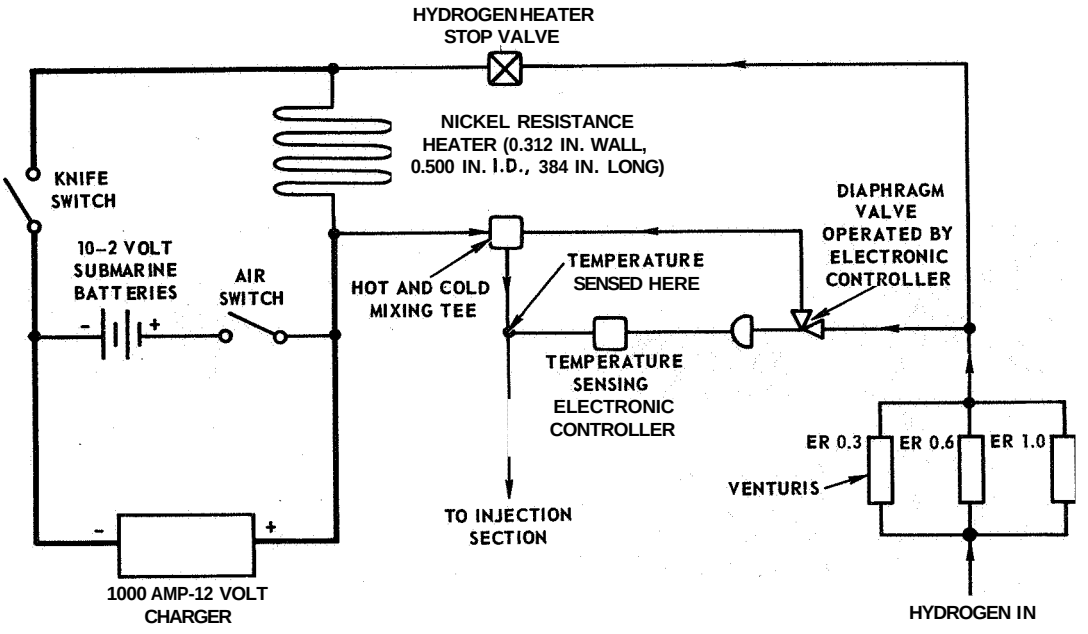

Fig. 6 SCHEMATIC OF HYDROGEN HEATER, ITS POWER SUPPLY AND CONTROL SYSTEM

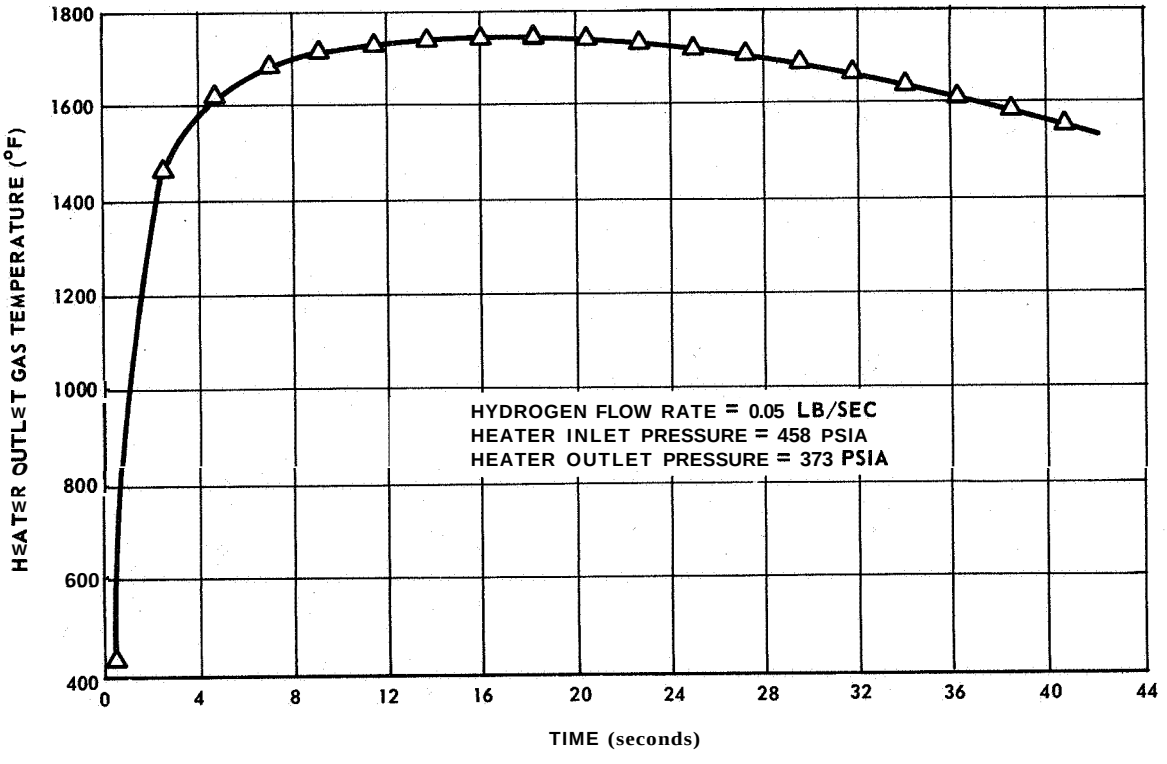

Fig. 7 HYDROGEN HEATER OUTLET GAS TEMPERATURE HISTORY

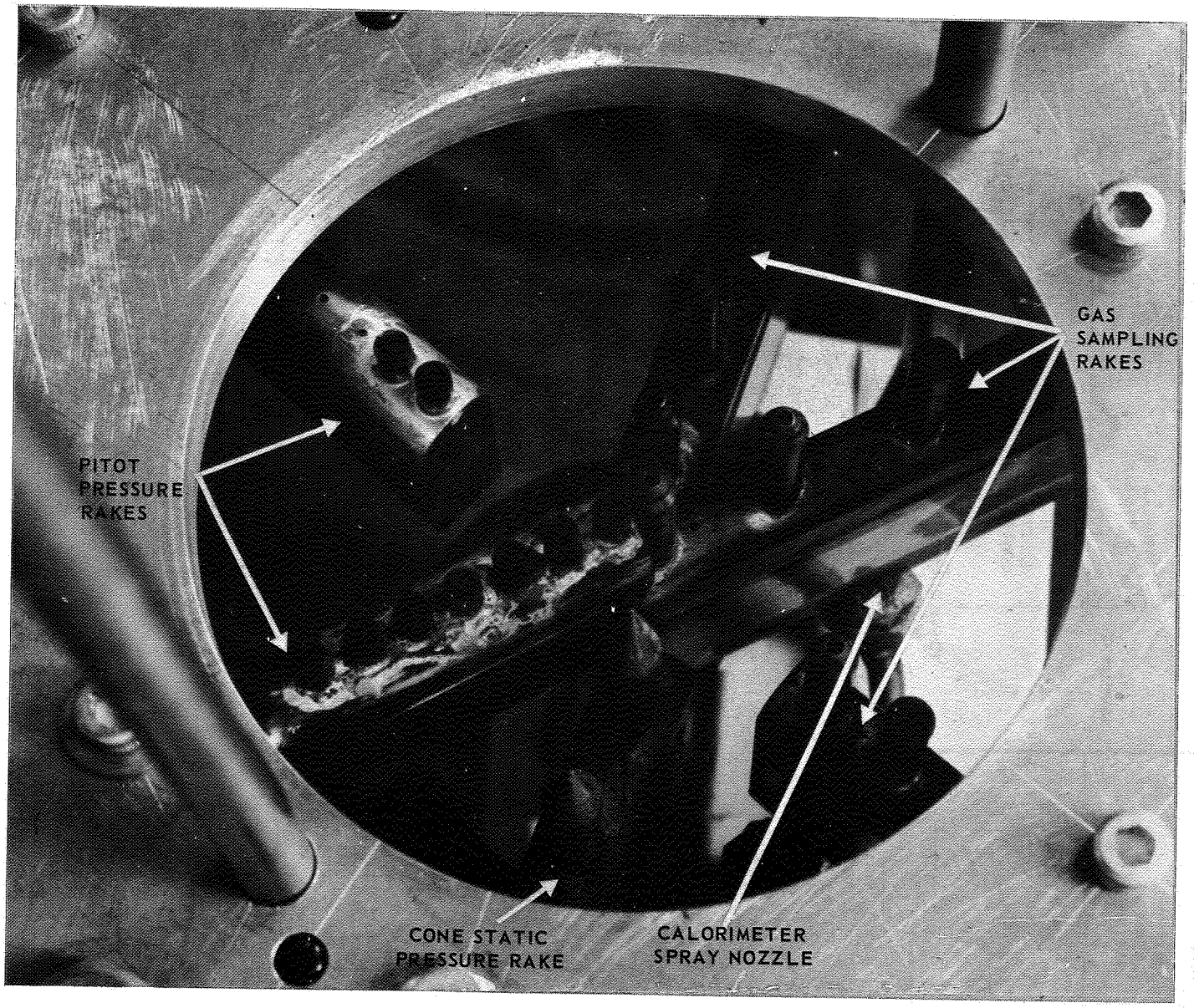

Fig. 8 COMBUSTOR EXIT PLANE INSTRUMENTATION

(A) GAS SAMPLE COLLECTION EQUIPMENT USED IN COMBUSTION TESTS

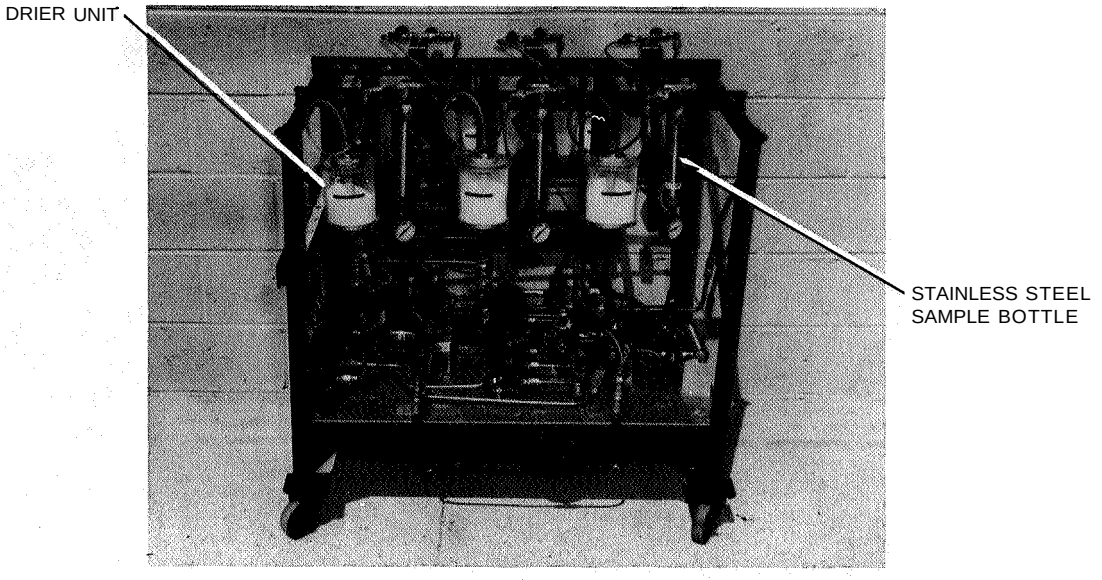

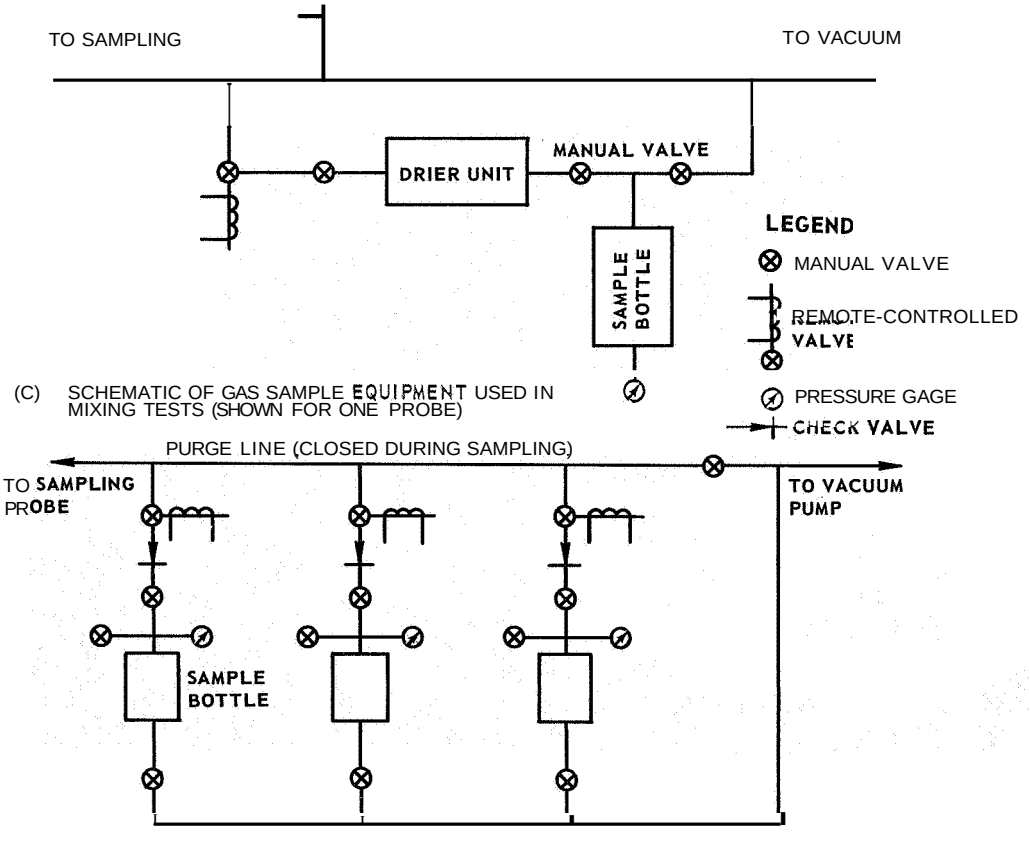

(C) SCHEMATIC OF GAS SAMPLE EQUIPMENT USED IN MIXING TESTS (SHOWN FOR ONE PROBE)

Fig. 9 GAS SAMPLE COLLECTION EQUIPMENT **USED** IN COMBUSTION AND MIXING **TESTS**

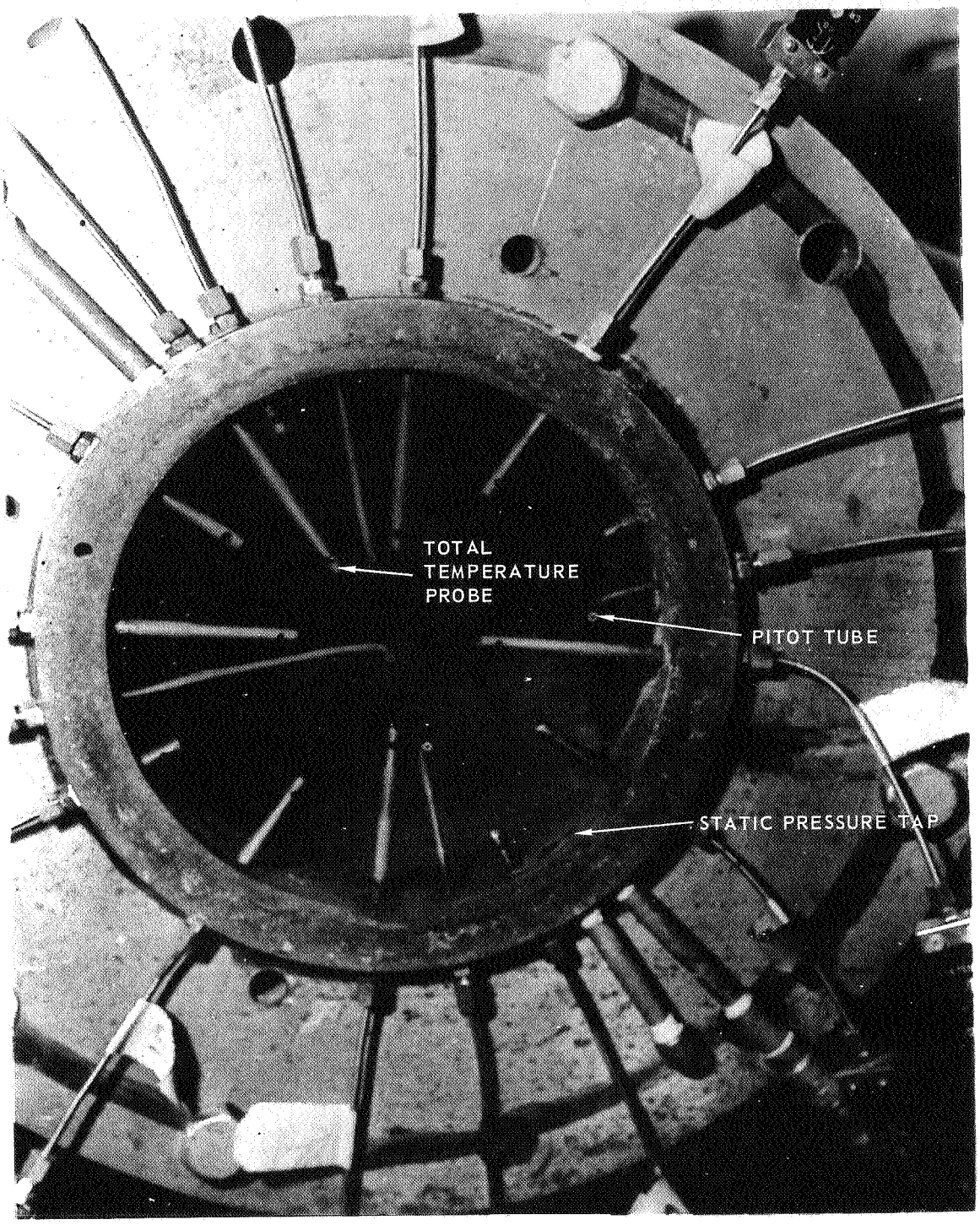

Fig. 10 INSTRUMENTATION IN CALORIMETER EXIT PLANE

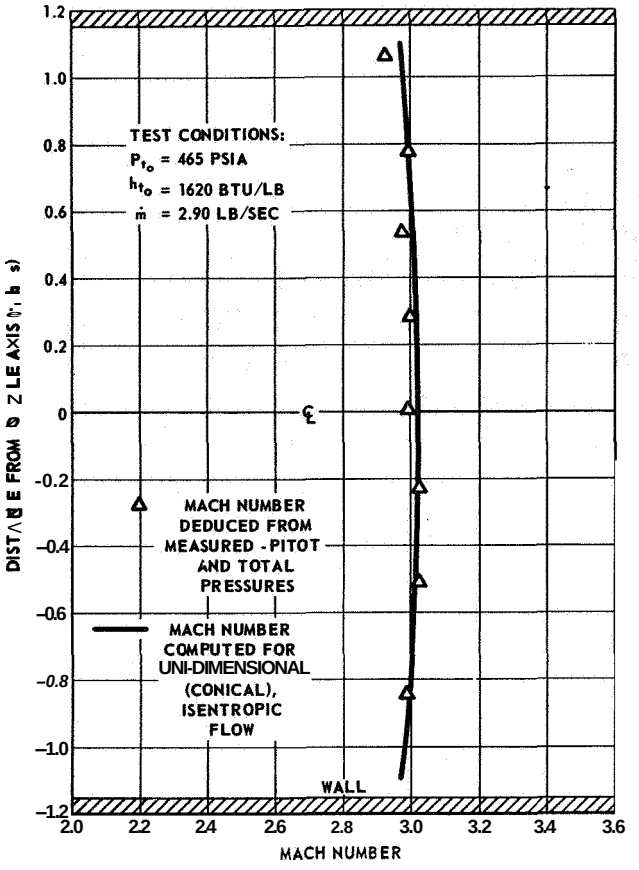

Fig. 11 MACH NUMBER DISTRIBUTION AT EXIT OF COMBUSTOR SUPPLY NOZZLE

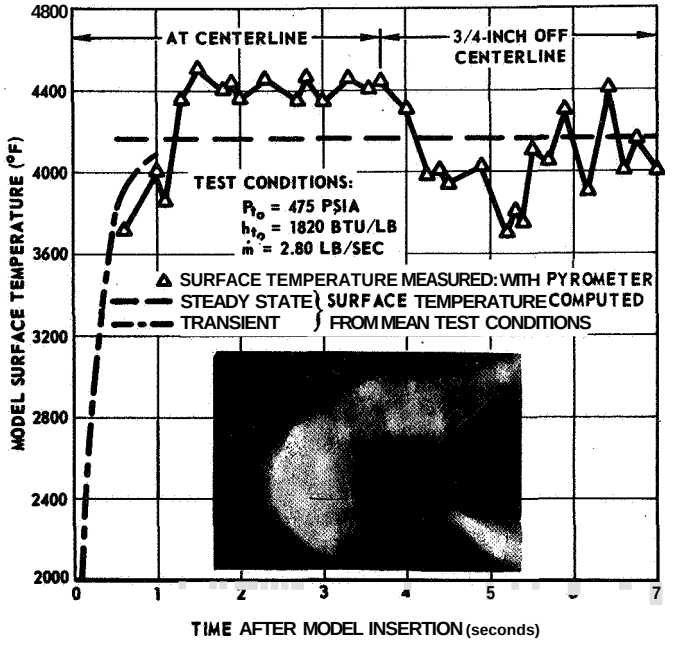

Fig. 12 TIME-TEMPERATURE HISTORIES AT TWO POINTS IN EXIT PLANE OF AIR SUPPLY NOZZLE AS INDICATED BY IMMERSED PROBE (SEE INSET)

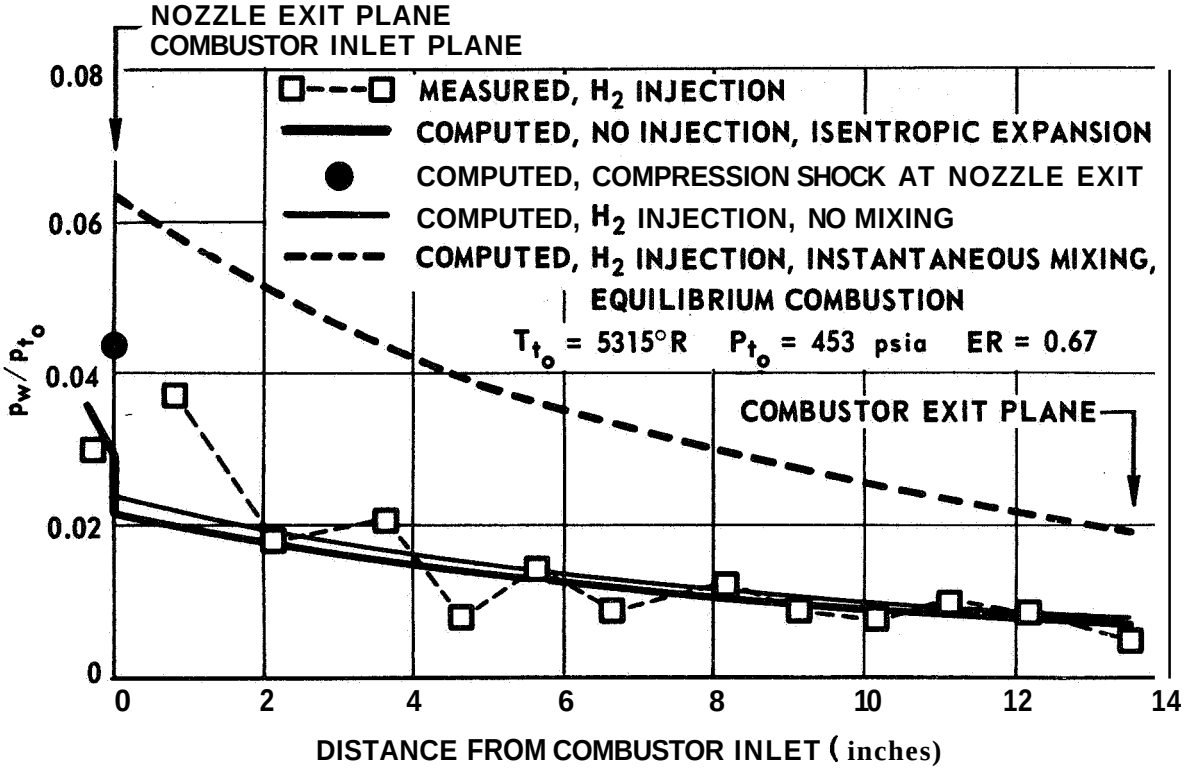

Fig. 13 COMPARISON OF THEORETICAL AND EXPERIMENTAL COMBUSTOR WALL PRESSURE DISTRIBUTION (RUN 2)

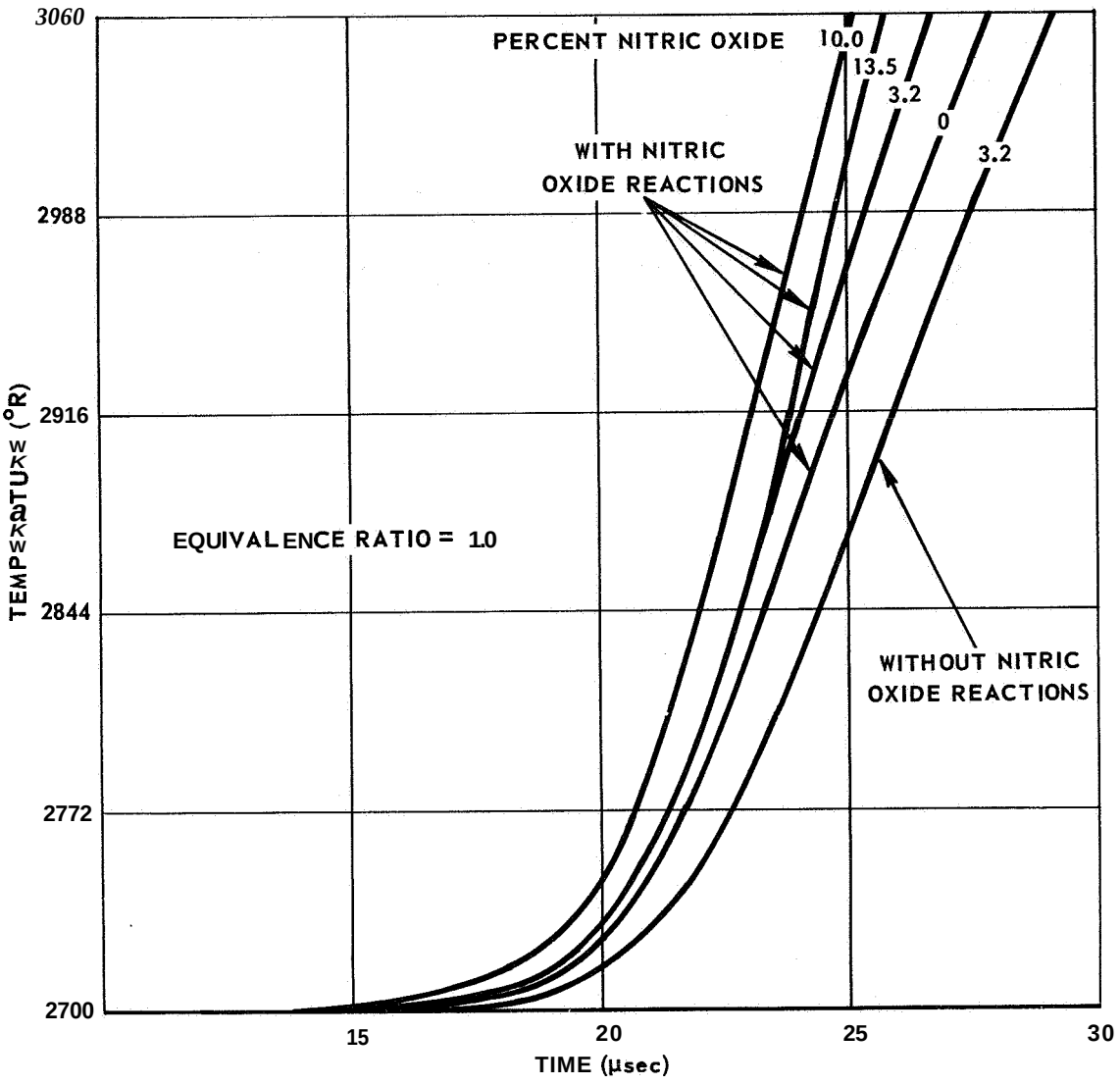

Fig. 14 EFFECT OF NITRIC OXIDE REACTIONS ON HYDROGEN-AIR CHEMICAL KINETICS

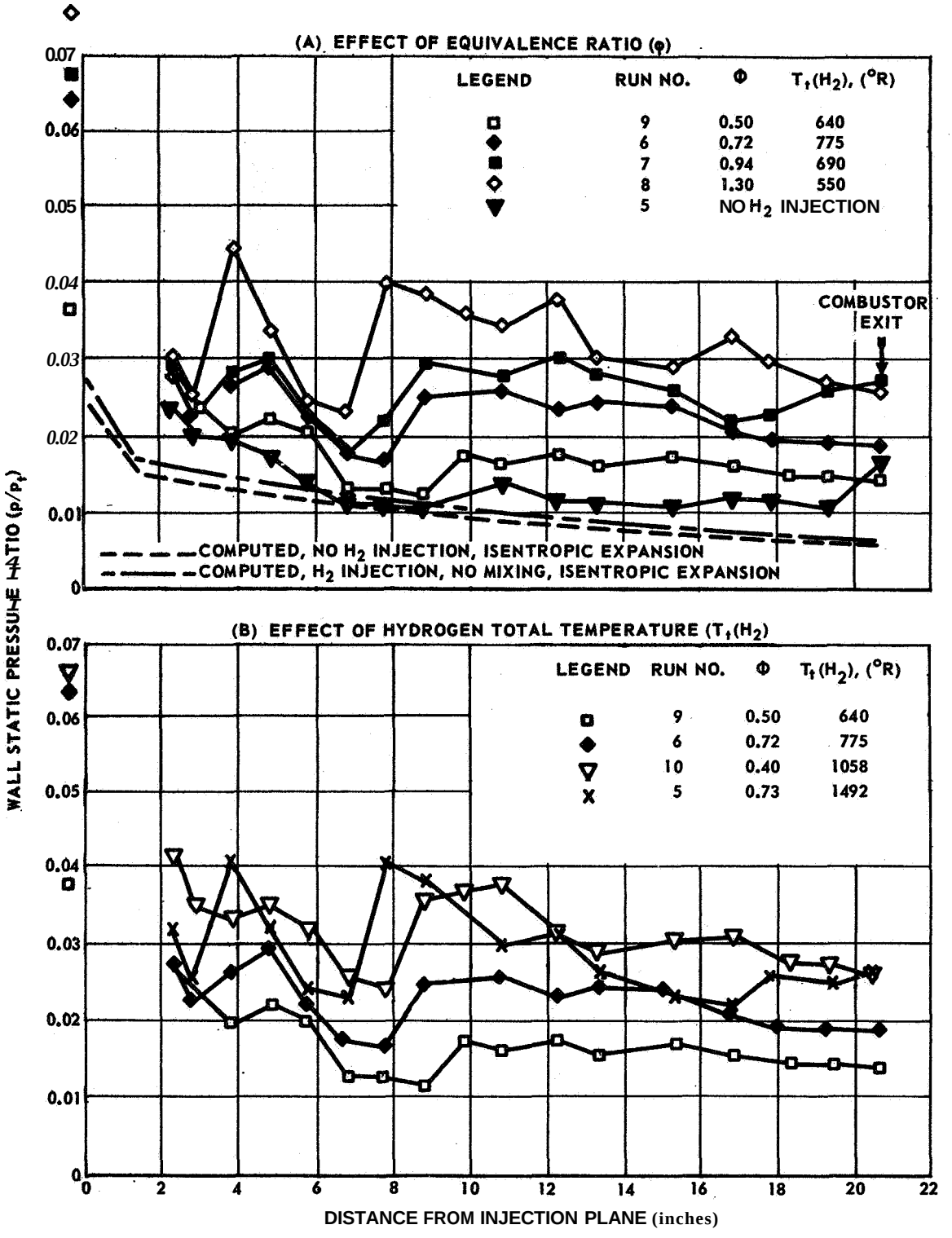

Fig. 15 EFFECTS OF EQUIVALENCE RATIO AND FUEL TEMPERATURE ON COMBUSTOR WALL PRESSURE DISTRIBUTION FOR 90°, 8-HOLE INJECTOR

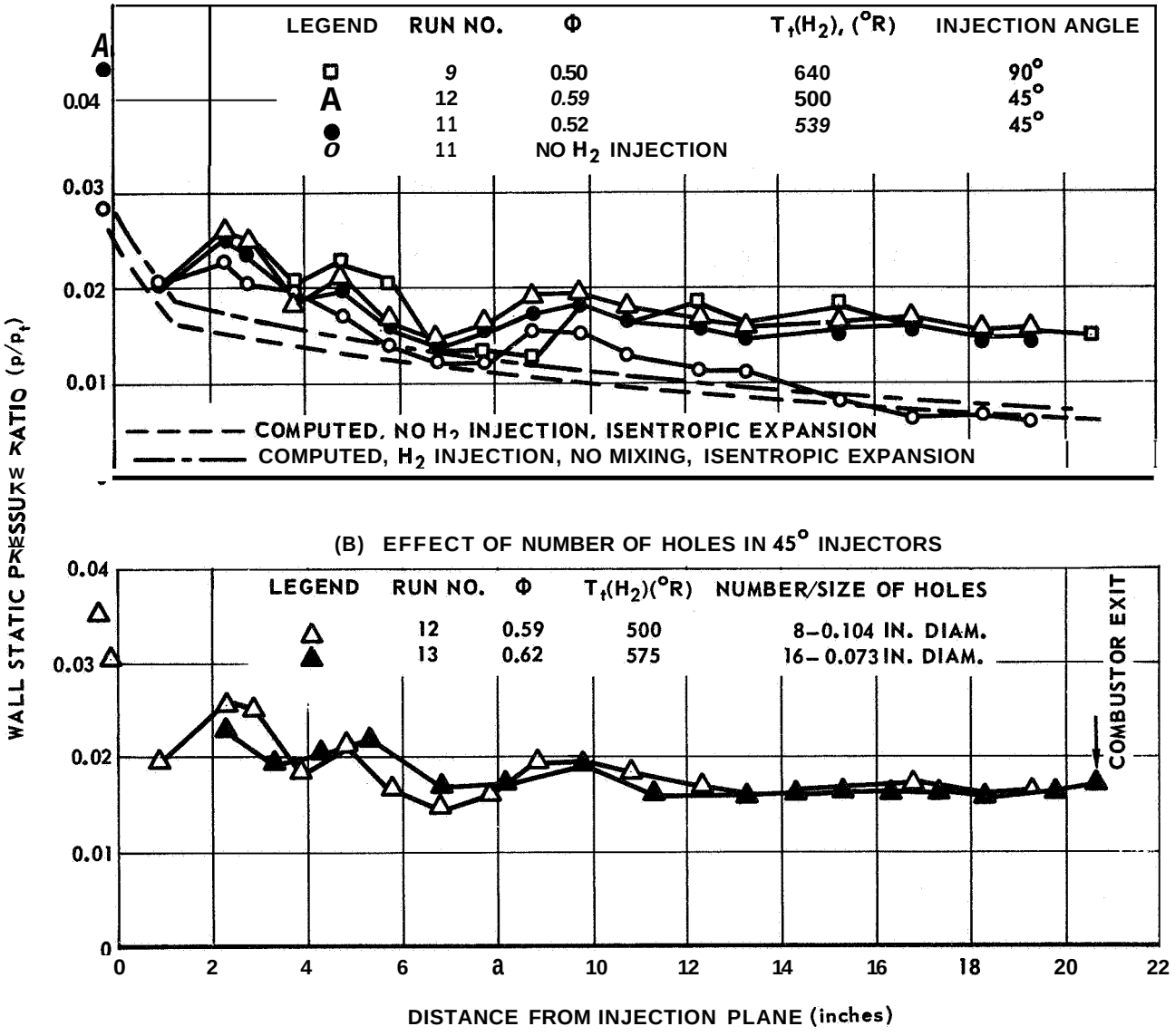

Fig. 16 EFFECTS OF FUEL INJECTION ANGLE AND NUMBER OF HOLES ON COMBUSTOR WALL PRESSURE DISTRIBUTION

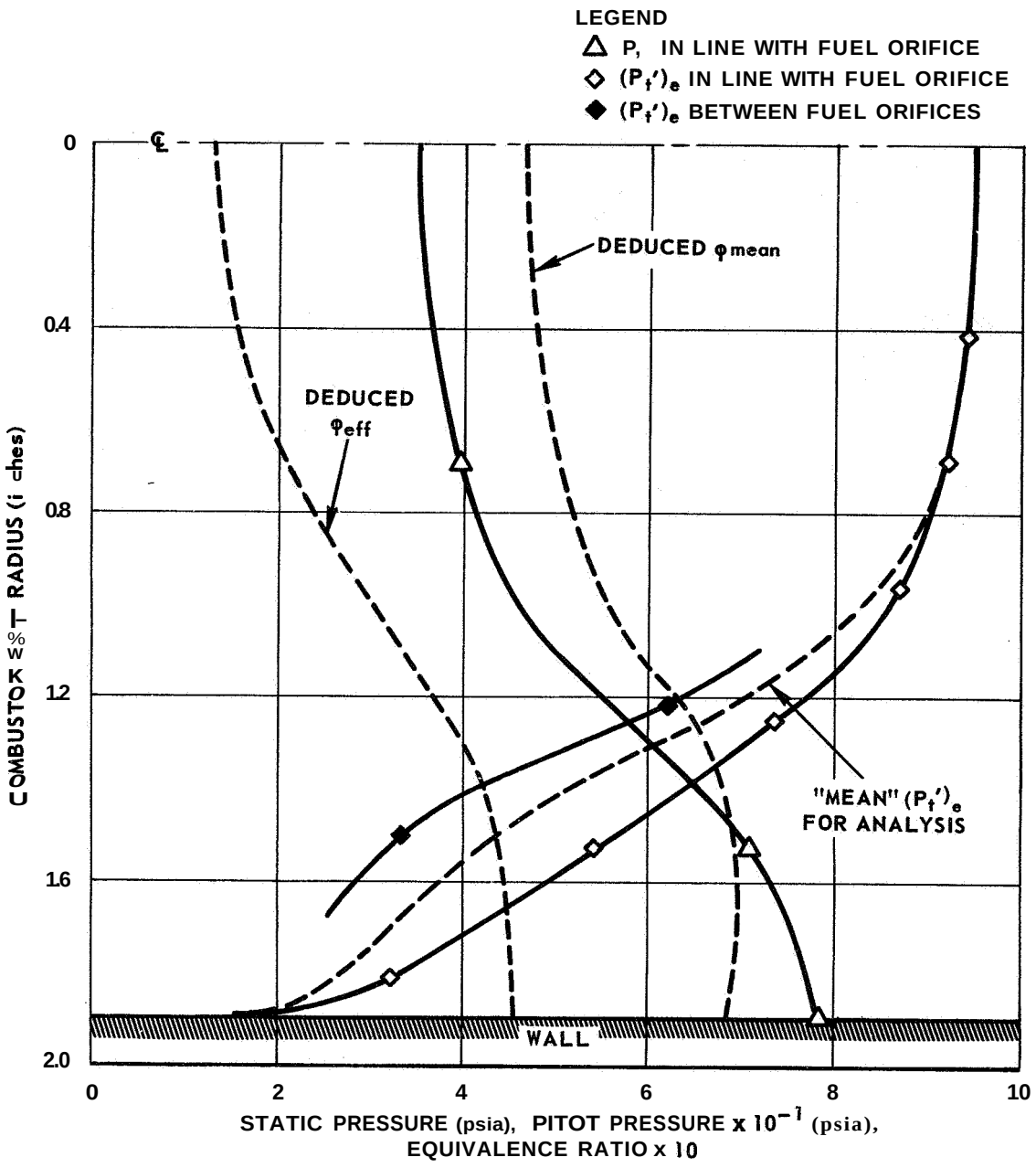

Fig. 17 EXPERIMENTAL AND ANALYTICAL PRESSURES AND EQUIVALENCE RATIO DISTRIBUTIONS (RUN 12)

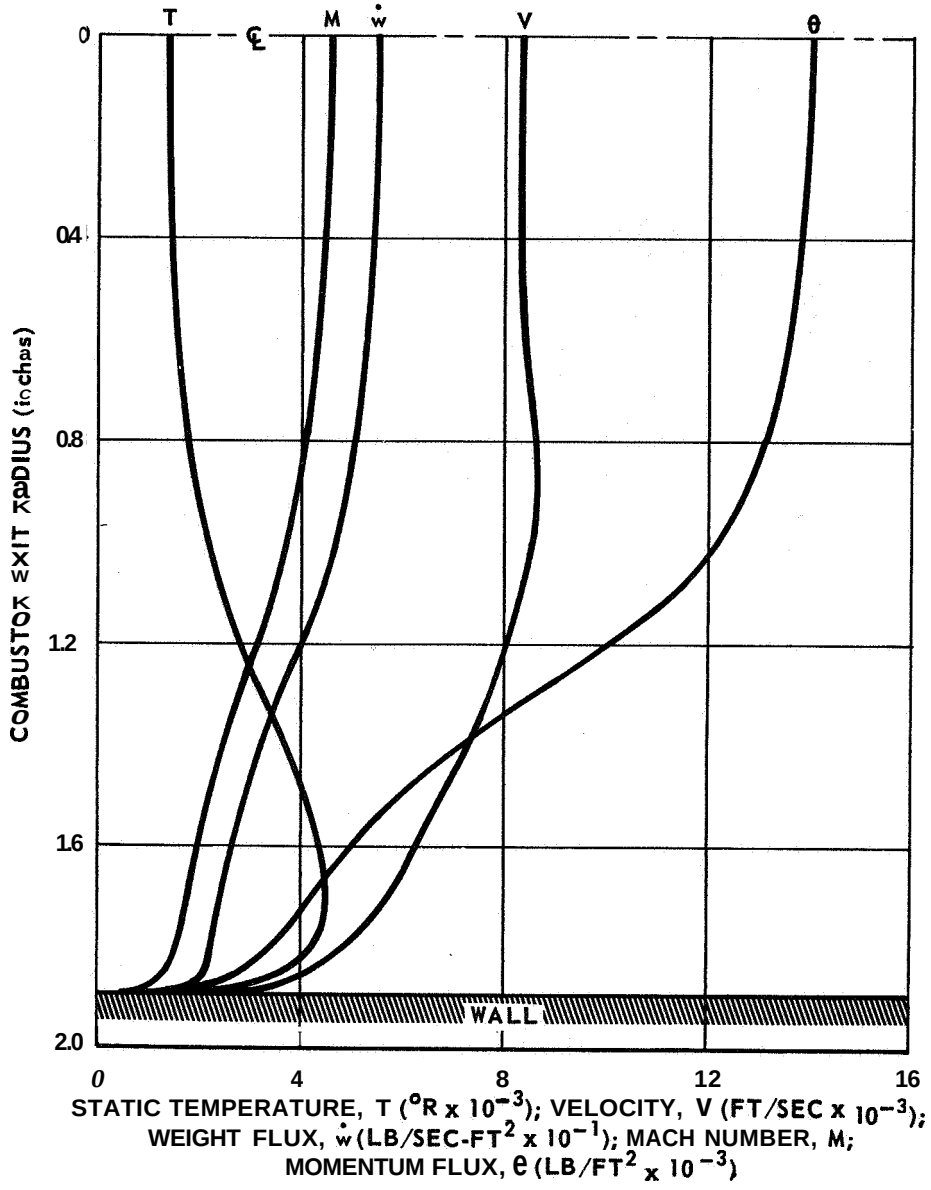

Fig. 18 DEDUCED FLOW PROPERTY PROFILES IN COMBUSTOR EXIT PLANE (RUN 12)

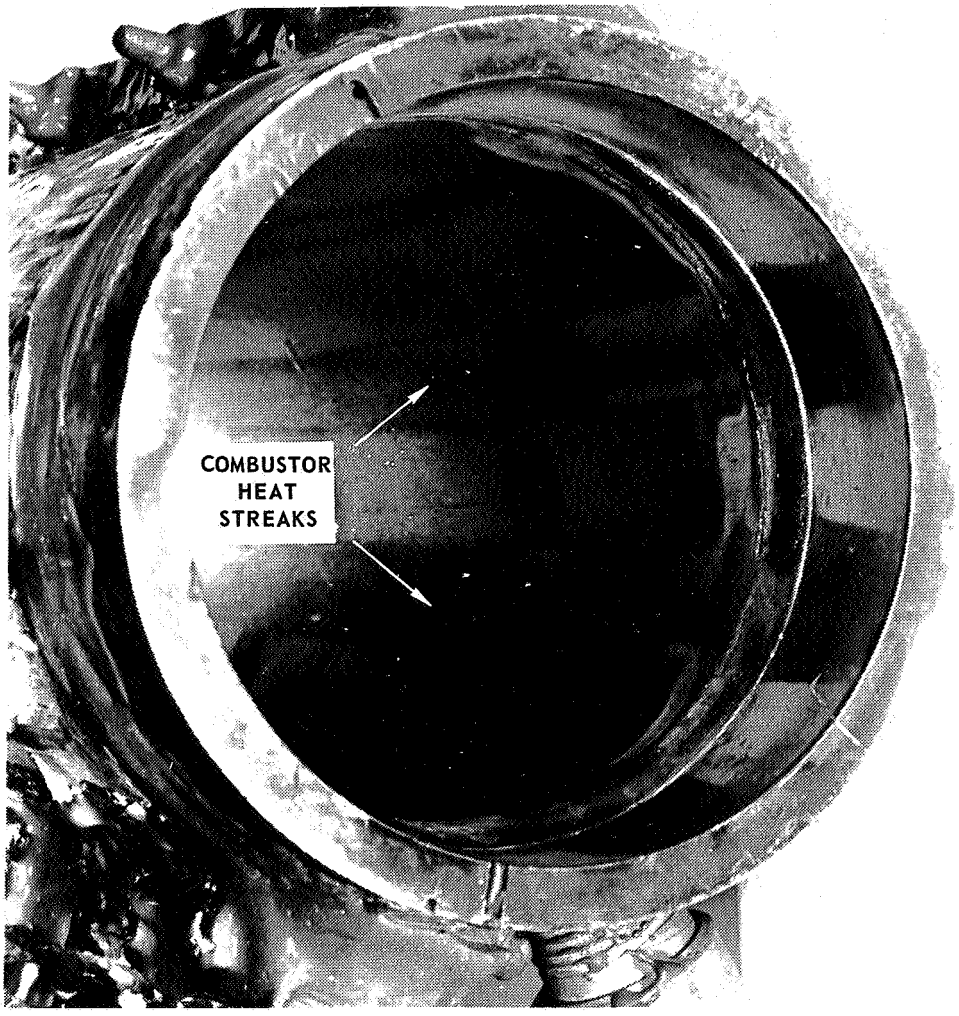

Fig. 19 DISCOLORATION PATTERNS ON COMBUSTOR WALL

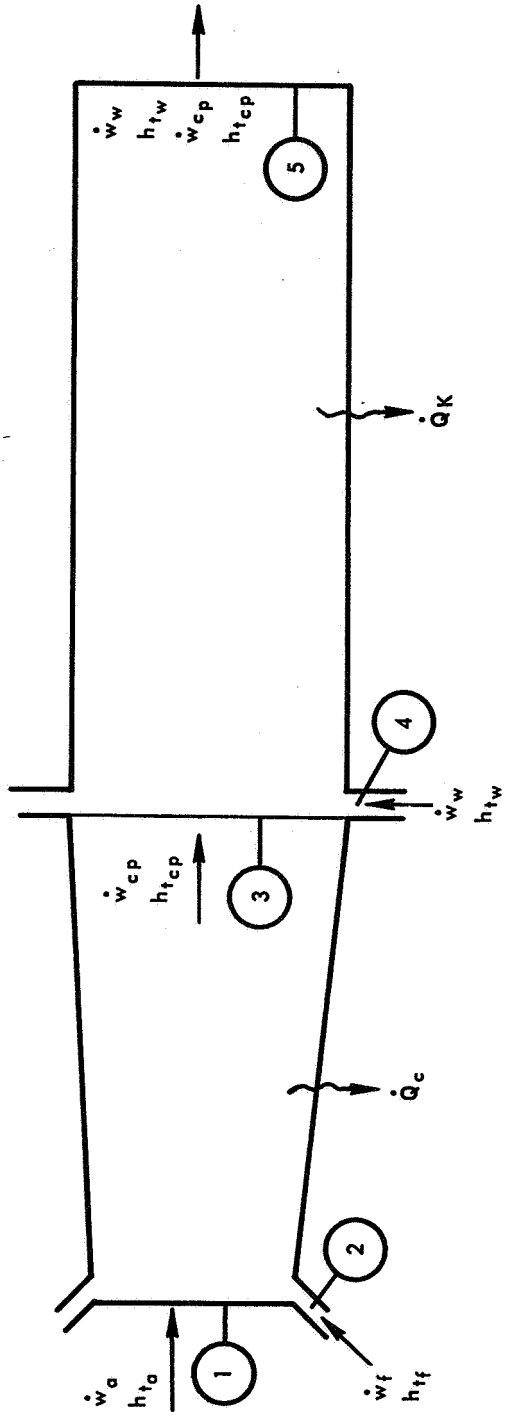

Fig 3-1 MODEL FOR DETERMINING COMBUSTOR-CALORIMETER ENERGY BALANCE

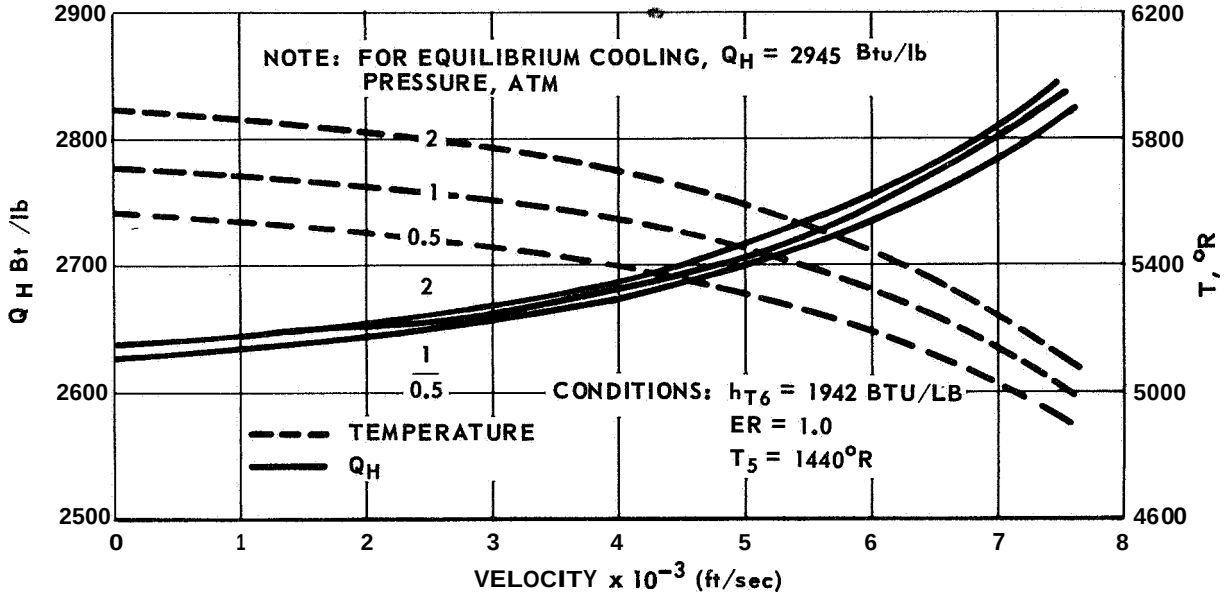

Fig. B–2 EFFECT OF COMBUSTOR EXIT CONDITIONS ON COMPUTED IDEAL HEAT RELEASE RATE

$T^{o}R$	$\rho(\mu\Omega cm)$	$\alpha(\mu\Omega cm/^{o}C)$
80	10.3	0.040
400	17.3	0.040
900	34.1	0.064
1800	46.5	0.023

Run	Combustor Inlet Conditions (Static)				Injectant Conditions (Static)				ER
	P_i (psia)	T_i (^{o}R)	$\dot{w}_i$ (lb/sec)	V_i (ft/sec)	P_f (psia)	T_f (^{o}R)	$\dot{w}_f$ (lb/sec)	V_f (ft/sec)	
1	13.2	2520	2.82	6800	17.5	490	0.041	1575	0.50
2	13.2	2520	2.82	6800	16.3	477	0.055	2180	0.67
3	14.5	2795	2.86	7002	14.5	261	0.091	6815	1.09
4	13.6	2542	2.85	6780	13.6	247	0.109	7125	1.31

TABLE III

Summary of Multiple-Hole Injector Tests

Run	Combustor Inlet Conditions (static					Injectant Inlet Conditions (static)					ER	(a) η_c %	β deg.	Number and Size Holes
	P_i psia	T_i °R	w_i lb/sec	V_i ft/sec	M_i	P_f psia	T_f °R	$\dot{w}_f$ lb/sec	V_f ft/sec	M_f				
5	11.2	2033	2.78	6409	2.97	145.8	1250	0.059	6564	1.0	0.73	125	90	8-0.104"
6	11.3	2001	2.82	6369	2.97	99.9	646	0.059	4725		0.72	70	90	8-0.104"
7	11.1	1909	2.85	6244	2.98	119.9	575	0.078	4461		0.94	85	90	8-0.104"
8	11.3	1989	2.84	6356	2.97	159.3	457	0.108	3998		1.30	62	90	8-0.104"
9	11.3	1990	2.84	6350	2.97	61.0	533	0.002	4300		0.50	61	90	8-0.104"
10	11.3	1948	2.86	6288	2.97	83.3	879	0.041	5501		0.49	72	90	8-0.104"
11	13.1	2553	2.81	6965	2.91	65.8	415	0.042	3821		0.52	72	45	8-0.104"
12	12.6	2410	2.80	6825	2.92	76.4	429	0.048	3879		0.59	68(b)	45	8-0.104"
13	11.4	2039	2.82	6415	2.97	93.9	479	0.051	4087	↓	0.62	64	45	16-0.073"

(a) Based on one-dimensional flow analysis.

(b) An η_c = 56% was calorimetrically measured in this run.